UNIVERSITY OF GÄVLE

FACULTY OF ENGINEERING AND SUSTAINABLE DEVELOPMENT
Department of Computer and Geospatial Sciences

Investigation of above-ground biomass with terrestrial laser

A case study of Valls Hage in Gävle

Mathias Billenberg

2023

Student thesis, Advanced level (Master degree, one year), 15 HE
Geomatics
Master Programme in Geomatics

Supervisor: Nancy Joy Lim
Assistant supervisor: Mohammad Bagherbandi
Examiner: Arash Jouvbari

Abstract

The thesis investigates above-ground biomass (AGB) with terrestrial laser scanning (TLS) for estimating AGB in a study area in Valls Hage, Gävle. The study used TLS for field measurements to collect highly detailed point clouds of two tree species for AGB estimation and comparison against validation data. TLS-derived data were validated using a non-destructive method involving direct field measurements using tape measures and a Trimble SX12 for extracting diameter at breast height (DBH), tree height, and crown diameter. Wood density was obtained from the literature. Data processing for segmentation, filtering, and generation of the quantitative structure model (QSM) was performed by using SimpleForest tool in Computree software. A statistical analysis was performed using linear regression, and AGB was estimated using QSM-derived volume multiplied by wood density. The finding in the results for the comparison of AGB estimation between TLS QSM and field validation from DBH-based tree-specific allometric equation had an RMSE of 154 kg, with a near-perfect agreement of 0.997 %, and RMSE of 189 kg, with the agreement of 0.990% for TLS QSM and TLS validation DBH-based tree specific equation. The comparison between TLS-derived DBH and field validation was accurate, leaving with insignificant differences, while the tree height had noticeable differences, and crown diameter had relatively low differences. The challenges during data processing were highlighted and the importance of TLS data for accurate AGB estimation, with the potential for refinement and integrating internal tree structure information to improve allometric models for future studies.

Keywords: TLS, tree species, QSM, AGB, volume, wood density, biomass, allometric, point cloud

Preface

I would like to express my gratitude to Nancy Joy Lim for assisting me throughout the study and providing access to the necessary equipment for field measurement.

Table of contents

1. Introduction

Greenhouse gases, such as carbon dioxide (CO_2), have increased rapidly and impacted global climate changes since the industrial revolution (Ledley et al., 1999). The main factor of greenhouse gases is human activities, for example burning fossil fuels in the industrial, which releases a large amount of CO_2. The increase of greenhouse gases results in global warming, which causes the earth's temperature to rise. Climate change affects human health due to events, such as floods, hurricanes, and extreme heatwaves (McMichael et al., 2006). In a way, it can have an impact on health problems, such as heatstroke and dehydration.

Forests have important role to reduce greenhouse gas emissions and mitigate the impacts of climate change (Chazdon & Brancalion, 2019). According to Chazdon & Brancalion (2019), tree restoration has big effects on the mitigation of climate change and reducing greenhouse gas emissions, especially CO_2. Trees also play an important role in carbon stocks, as they can absorb CO_2 from the atmosphere, and the size of carbon stocks is determined by tree diameter and forest structure (Pragasan, 2020). Forest structure can be referred to as density, height, and spatial distribution.

Above-ground biomass (AGB) refers to all living biomass, such as tree stumps, branches, seeds, leaves, and other plant materials (Kumar & Mutanga, 2017). AGB can be estimated through non-destructive or destructive method. The destructive method is a method that involves damaging or harming trees, i.e. cutting down trees or vegetation. The non-destructive method involves no harm to the trees or vegetation and is often done through remote sensing survey, ground-based survey, and allometric equations. Allometric equations are the key for estimating tree dimensions, such as diameter at breast height (DBH), wood density, crown area, and tree height (Návar, 2009), and are useful for accurate biomass estimation. Overall, AGB is a main factor to estimate carbon stock and determining the tree's characteristics.

DBH is a measurement that is the most used parameter for estimating the diameters of a tree trunk with a standard height of 1.3 meters above the ground (Kuyah et al., 2012). The reason for the standard height is due to the tree's roots or branches, which would affect the results of measurement. Thus, measuring at this standard height would ensure a more accurate measurement for estimating AGB.

As stated above for the non-destructive method, remote sensing, and ground-based survey can be used to estimate AGB. Remote sensing survey refers to using satellites to estimate biomass, which is then based on vegetation information, such as NDVI (Normalized Difference Vegetation Index). NDVI can be used to provide information on the amount of health status of the vegetation and is useful for large-scale assessment (Kumar & Mutanga, 2017). However, to estimate AGB more accurately, the ground-based survey is often preferred. Furthermore, it is also widely used for gathering inventory data of trees, such as extracting tree attributes, capturing 3D forest structures, and monitoring tree growth.

Ground-based surveys often use tape measures or laser-scanning surveys to measure directly on the field for the individual tree dimensions, such as DBH, wood density, and

tree heights. A laser scanning survey, also known as Light Detection and Ranging (LiDAR) is a technology that uses a pulse of energy to measure an object's distance from the earth's surface to the sensor (Wandinger, 2005). In a way, LiDAR can generate highly detailed and accurate three-dimensional point clouds. According to Liang et al., (2012), LiDAR has been proven to be useful for direct measurement on the field to estimate DBH and tree heights, and able to distinguish different tree species.

There are two main types of LiDAR, which are airborne laser scanning (ALS) and terrestrial laser scanning (TLS). ALS is used to gather 3D information to generate 3D point clouds and provides more accurate information about vegetation or terrain elevation for large areas (Wehr & Lohr, 1999). However, it is not that useful for detailed structured information for the trees. TLS is an instrument that uses LiDAR to gather 3D-point clouds from the surrounding area on the ground (Liang et al., 2016). TLS can, therefore, obtain more detailed structured information compared to ALS.

The Quantitative Structure Model (QSM), developed by Raumonen et al. (2013), can be used to generate a complete 3D model of trees from the point cloud data, usually taken from TLS or remote sensing technology. The model consists of individual segments of tree structures, such as stems and branches, and are commonly used to estimate tree volume, biomass, and carbon stocks.

1.1 Aim and research questions

The aim and objectives of this study are to estimate carbon stock from AGB using TLS. TLS is then used to collect 3D-point cloud data of individual trees from a specific area in Valls Hage, Gävle. The 3D-point clouds are used to estimate tree dimensions with the choice of different allometric equations, which are DBH, tree heights, and crown diameter. Wood densities are taken instead from literature studies, as the aim is to avoid using the destructive method. The validation of accuracy from the TLS measurement will be done with the direct measurement using a tape measure, and total station survey, to ensure reliability.

The research questions, related to the aims and objectives of this study consist of the following:

1. What are the key challenges and considerations in processing TLS data for obtaining tree attribute parameters to estimate AGB?
2. How varied and accurate are the AGB estimations for the TLS-derived data using the allometric equations using the DBH, and QSM model (volume × wood density), when compared to the field validation data?
3. How can QSMs be used for other purposes other than estimating AGB?

1.2 Delimitation

A specific area in Valls hage, consisting of two different tree species will be focused, primarily due to time-limitation. The study will only rely on non-destructive method, avoiding the need for destructive sampling. Instead, existing allometric models from literature studies or databases in Sweden will be utilized.

2. Theoretical framework

2.1 Above-ground biomass

As accurate estimation of carbon stocks is necessary for non-destructive and destructive methods, it is also crucial to have a great understanding of the AGB. A study by Houghton et al. (2009) emphasizes the role of biomass in the global carbon cycle, where carbon is cycled between the earth's atmosphere, oceans, and land. Carbon is the main element for all living organisms and plays an important role in the ecosystem. According to the authors, biomass accounts for 50% of the carbon stored in AGB and the remaining 50% in dead biomass, such as fallen trees and logs. Therefore, trees play an important role in absorbing carbon from the atmosphere, which is performed through photosynthesis, a process where carbon, water, light energy is converted into oxygen. The amount of carbon stored in the biomass is dependent on the size and growth rate of the trees. Therefore, larger trees have a greater capacity for absorbing carbon and accumulating biomass, thus, could mitigate climate changes (Pragasan, 2020). The loss of biomass from land use changes, fire forest, and deforestation contribute to climate changes and global warming by releasing greenhouse gases into the earth's atmosphere. Therefore, both monitoring and measuring of the AGB are necessary to develop a better understanding of the role of biomass in the carbon cycle. Methods such as remote sensing and ground-based survey are necessary for estimating the AGB accurately.

2.2 Factors affecting AGB estimations

The factors affecting AGB estimations can be influenced for instance by tree attributes or parameters, tree species, and climatic factors. Thus, studying and understanding these factors are essential for an accurate AGB estimations.

The tree parameters, including DBH, tree height, and crown size are influenced by various climatic conditions, and plays a crucial role for accurately estimating AGB. The climatic conditions, such as sunlight, temperature and precipitation impact the tree growth rates and AGB accumulation (Chave et al., 2014). Larger trees generally contribute more to the accumulated AGB due to the size of DBH, height and crowns. These parameters are essential as variables for the allometric equations, which is commonly used to estimate AGB. Therefore, the relationship between tree parameters and climatic factors is consistent and plays a crucial role for developing allometric models for AGB estimations.

When considering AGB estimation, it is also essential to consider the different species' characteristics. Each tree species has its own specific wood density, which influences the accuracy of AGB estimation (Chave et al., 2009). Wood density is a crucial parameter in allometric equations for estimating AGB due to the relationship of the carbon storage in the tree's biomass.

2.3 Different methods for estimating AGB

Various methods for estimating AGB are available, including ground-based survey and remote sensing techniques. Ground-based survey methods can be performed through traditional field measurement for extracting tree attributes, such as DBH and height, thus, utilizing allometric models to estimate the AGB (Miah et al., 2020). According to Miah et al. (2020), the allometric models are derived from the destructive method, meaning trees were felled, cut, and processed for the calculation of DBH and tree height. The authors first measured DBH by using a caliper, with a standard height of 1.3 m above the ground on the tree stems before felling the tree. After felling, tree height was measured by using tapes, as it is more convenient to measure on the ground. Samples of different parts of tree species, such as branches and leaves are then used to calculate the fresh and dry biomass. Dry biomass is often used to estimate carbon stocks after being dried out and fresh biomass is used to estimate the water content directly after collected samples. The authors then developed four different types of allometric models, based on DBH and tree height, and used a combination of simple and multiple linear regression analysis for the result.

A case study in Sweden utilized a method for the biomass functions in the SKA 99 project, which are used to estimate biomass for different tree species, such as pine, spruce, and birch (Petterson, 1999). The biomass function relies on describing both volume and wood density components of biomass, where the volume considers factors such as DBH, and height, while the wood density component corresponds to the tree's growth and age. Furthermore, the author collected the sampling data of forest conditions from the *Swedish National Forest Inventory* and used a multiplicative regression model, a type of mathematical equation, to describe the relationship between variables and estimate biomass. The variables that were used in the functions include soil type, location, DBH, and age. Finally, the author further emphasizes the usefulness of estimating biomass from the biomass functions with high precision.

For broad-scale assessment to estimate AGB, remote sensing technology has advantages as a method. A study by Kumar & Mutanga, (2017) highlighted the use of remote sensing technology. The authors emphasize the advantages of using remote sensing over traditional methods of measuring AGB, such as cost and time-effectiveness and less impact on climate change. Three different types of remote sensing data are commonly used for biomass estimation:

1. Optical sensor provides broad-scale coverage for vegetation measurement, which is often used to estimate vegetation indices, such as NDVI. They are limited by clouds and not able to penetrate through vegetation.
2. Radar can penetrate through vegetation due to electromagnetic waves, which provide detailed vegetation structures. This type of data is useful for detailed vegetation structures, such as stem density. Radar data have lower resolution and accuracy compared to LiDAR.
3. LiDAR provides accurately detailed 3D data with high resolution for vertical structures and height measurement of forests but is limited by clouds and can be expensive.

Another method of remote sensing technology is the utilization of the Random Forest (RF) regression algorithm in Southern China (Wang et al., 2016). The authors used a machine-learning algorithm for estimating wheat biomass from remote sensing data. The RF algorithm is built on multiple decisions trees to handle complex relationships between input variables (wheat biomass) and the target variables (vegetation indices). The RF was compared against machine-learning algorithms of support vector regression (SVR) and artificial neural network (ANN). The results indicate that the RF model was more accurate in the estimation of wheat biomass compared to SVR and ANN.
The challenges suggested by uncertainties in field reference data can significantly impact remote sensing studies (Persson et al., 2022). The authors emphasize the uncertainties and errors when assessing the accuracy of biomass estimation using ALS in Scandinavian forests. Therefore, this article focuses on the uncertainties from reference field data, including model errors, position errors, and measurement errors, which can affect the accuracy of biomass estimation. To address these challenges, the authors introduced a theoretical framework, namely the error characterization model (ECM). ECM can be used to quantify and characterize the errors to provide a better understanding and adjustments to improve the accuracy of biomass estimations.

2.4 Terrestrial laser scanning

Another method for ground-based surveys, other than the traditional field measurements, is utilizing TLS, which offers several advantages as a non-destructive method. This technology allows for the rapid capture of millions of points in point cloud data, capturing highly detailed information on tree inventory data, such as DBH and tree height (Liang et al., 2016). Additionally, TLS can distinguish different tree species based on the tree's characteristics in the point cloud data.

However, the disadvantages of TLS include the cost and equipment requirement, time-consuming processing of data, and occlusion gaps (Newnham et al., 2015). The Newnham et al. (2015)emphasize the difficulties in dense vegetation due to occlusion and the need of merging scans, which can be time-consuming. Furthermore, using TLS to extract tree attributes can introduce noise and affect the accuracy of the AGB estimation due to factors such as site conditions, and forest and tree structure (Xu et al., 2021). This means that complex topology (e.g. rough terrain), and adverse weather conditions (e.g. strong winds) can affect the quality of the TLS data. In addition, dense canopies, and overlapping branches can lead to incomplete scans or errors in identifying trees.

Finally, TLS is not limited to extracting basic tree inventories, but can also be utilized for visualizations purposes. For instance, Calders et al. (2020) utilized TLS to assess and study the complexity of the structure of trees, such as the shape and size of the canopy. In general, TLS plays a crucial role in forest ecology research, due to the ability to measure and analyze the forest area (Danson et al., 2018), and provides researchers a more comprehensive understanding of forest ecosystems.

2.5 TLS and AGB estimation

To mitigate climate change and reduce greenhouse gas emissions, accurate data is necessary to estimate the AGB. An article by Demol et al. (2022) provided an overview of using TLS to estimate forest AGB and further discussion with the potential of using TLS in the future. The authors collected ten previous studies to re-analyze the TLS-derived AGB estimation results with coverage of the forested continents, and include both destructive and non-destructive methods. Non-destructive methods involve field measurements, in this case, TLS, to collect point cloud data. Point cloud data was then processed using software for filtering and extracting attributes from individual trees, such as DBH, tree height, and the crown of the tree. The attributes are then used for estimating tree volume and AGB. The destructive method was used for the validation purpose from the TLS-derived data and involves tree harvesting for sampling and weighting the stem, leaves, and branches for measurement and to estimate AGB. Lastly, the comparison between TLS-derived data and validation data is shown to be accurate for estimating AGB. However, the authors argued that TLS has some limitations for estimating AGB due to the high cost of the instrument and the time-consuming post-processing data.

A study case in Germany, using the TLS for urban trees was also highlighted by Kükenbrink et al. (2021). The authors focused on the TLS measurement to estimate AGB and includes both non-destructive and destructive methods. For the non-destructive method, the authors used TLS for collecting point cloud data and extracting tree attributes, such as DBH, tree height, and crown area. For the wood density estimation, the authors used literature studies. Wood volume was calculated from the extracted tree attributes by using the QSM tool in MATLAB software. AGB was then estimated by multiplying the wood volume, extracted from the QSM, with a specific wood density. The destructive method was also used for validation purposes, which involves tree felling for sampling and weighting to determine wood density. A tape measure was used for the DBH measurement and a rangefinder instrument for the crown area and tree height. AGB was estimated by the allometric equations. Lastly, both AGB, from TLS-derived and from reference measurement, was compared by using the linear regression analysis. The author pointed out that crown areas were the most important factor for estimating AGB, followed by DBH and tree height.

2.6 Tree reconstruction

Tree reconstruction involves the process of generating 3D geometric and topological structure of a tree from point cloud data, usually obtained from TLS. This is known as QSM and can be used to provide detailed information about the tree's structure (Raumonen et al., 2013). The reconstruction process of the tree is approximated by fitting cylinders, representing the shape and orientation of the segment. Therefore, the process begins with a starting point cloud and extends to the end of point cloud of the segment, generating a cylinder corresponding to the segment. These cylinders can be optimized through the utilization of least squares method. By combining these optimized cylinders, the complete tree structure can be reconstructed. This is usually performed through algorithms and computations, commonly in software like MATLAB, used to

identify geometric shapes and topological orders based on the major branches and the main trunk.

An example of algorithm is referred to the *Neighbor-Relation Segmentation Algorithm*, which is used to separate a tree component into individual parts (Raumonen et al., 2013). This algorithm identifies bifurcations, where a single branch divides into two or more branches, and utilize these bifurcations to determine the structure of the tree accurately.

Finally, the QSM can then be utilized to extract basic information about the tree. This includes information on total tree volume, branch volume, the number of branches, and the size dimension of the cylinders. Additionally, measuring distance or angles from branches can be obtained. These information could be useful for forest applications, forest ecology, AGB estimation, refinement of allometric models, and visualization purposes (Fan et al., 2022; Fekry et al., 2022; Gonzalez de Tanago et al., 2018). In summary, QSM represents a comprehensive representation of the tree structure, including the extraction of basic information for further analysis and estimating AGB.

Reconstructing and computing tree model can be difficult that requires expertise. Therefore, a more automated and user-friendly approach, using a software tool SimpleForest, was developed by Jan et al. (2021). The tool is used within the Computree platform, which is a software package for processing and analyzing point cloud data (Computree Core Team, 2022). Furthermore, SimpleForest is built on the principles of QSM, which utilize TLS of forest plots to convert to a cylinder-based 3D model. Thus, the main difference between QSM and SimpleForest QSM is that it has an automatic algorithm for sub-segmentation, which involves dividing the tree components into different parts. In contrast, traditional QSM involves using manual algorithms for segmenting and filtering the trees. These methods aim to reconstruct the point cloud trees into 3D-cylinder model, with the following common step:

1. Tree cloud filtering and segmentation focuses on filtering out unwanted noises and converting point cloud into segments corresponding to individual tree, such as stem and branches.
2. QSM reconstruction involves utilizing various QSM methods, such as *spherefollowing* to fit cylinders into a tree cloud. Additionally, inputs like the *median filter* are utilized to correct the over- or underestimated cylinders. The process also utilizes *refit cylinders* to align points to the closest cylinder, and *wellfit cylinder* to classify the quality of the fit as either well or bad. Allometric correction as the final step is commonly used to detect incorrectly fitted cylinders and apply suitable correction using various parameters.

For instance, Hackenberg et al. (2022) emphasize the accuracy of the wood volume estimation using SimpleForest, and a comparison was conducted against another QSM tool, namely TreeQSM. The comparison involved filtering the QSMs generated from tree clouds and correcting overestimated radii. Then, the corrected QSM volume was compared against harvested reference data of 66 felled trees. According to the authors, the results of the comparison indicate a significant improvement in accuracy using the SimpleForest tool compared to TreeQSM.

However, there are instances wherein measuring the diameter at the tip of the tree can be challenging when it comes to predicting biomass, by combining volume with wood density (Hackenberg et al., 2015). Hackenberg et al. (2015)suggest that all tree compartments with a diameter smaller than 4 cm are often overestimated in prediction and can vary the biomass estimation. Furthermore, compartments larger than 10 cm in diameter are more likely accurate.

As TLS is more commonly used, along with highly detailed information on tree point clouds and QSM, the need for extracting tree attributes from individual trees is necessary to obtain their DBH, tree height, and detailed crown areas. That is where the open-source R-script comes in, along with the assistance of various packages to perform the function. The R package *Individual Tree Structural Metrics* (ITSMe, *https://lmterryn.github.io/ITSMe/*.) has been provided to obtain tree attributes automatically from individual tree points and QSMs (Terryn et al., 2023). In addition, these attributes provide important information, such as the size, structure, and volume of individual trees.

3. Methods

The overall workflow of the study was presented in Figure 1. It began with field measurement for both TLS and validation data. Next, the TLS data was processed for filtering and segmentation. Followed by extraction of the tree attributes from TLS data and a QSM was reconstructed. Subsequently, statistical analyses were conducted on both the TLS and validation data to obtain the results.

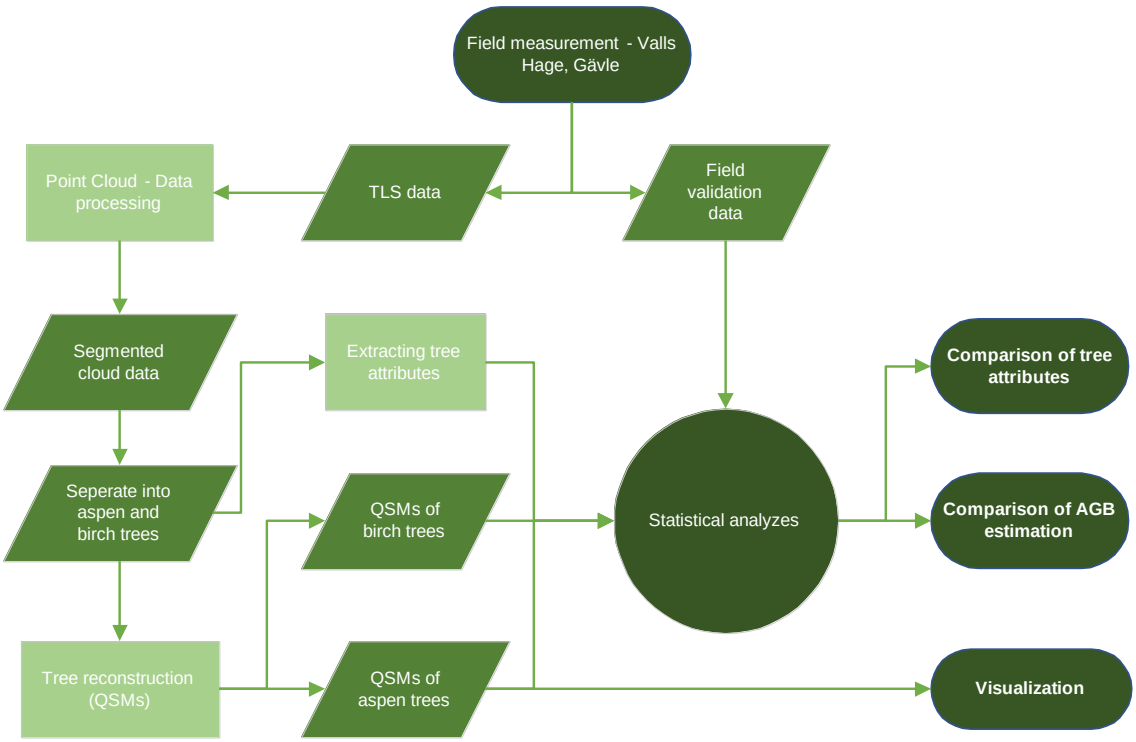

Figure 1. The workflow

3.1 Study area

The study area, Valls Hage, is located in the city of Gävle, Sweden (figure 2). Valls Hage is a forest botanical park, which covers around 10 hectares in size and consists of over 200 different tree species (Gunnarsson & Lorentzon, 2017). The specific area in Valls Hage was conducted in the southern part of the area (figure 2, red arrow) with two dominant tree species, aspen (Populus tremula) and birch (Betula bendula). The reason for choosing these two dominant species is due to their differences in growth pattern, tree structures, and wood properties, which makes it suitable for analyses.

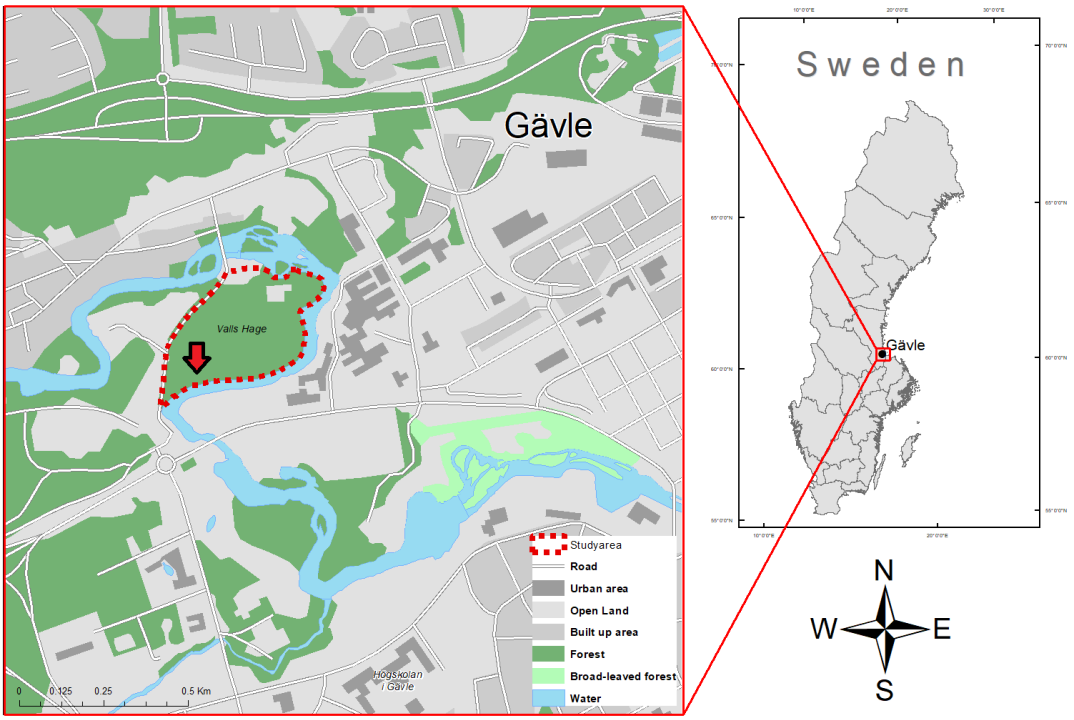

Figure 2. The right side shows a map location of the city of Gävle, Sweden and the left side shows the study area at Valls Hage (Red dotted line) in Gävle. Coordinate system: SWEREF 99 TM

3.2 Materials and data

The materials that were used for the study were a TLS instrument, specifically, the Trimble SX12 (see table 1 for specifications), and a tape measure. Trimble SX12 is an effective multi-station instrument for collecting accurate 3D data for forestry applications, as it can capture data effectively, with a scan rate of 26,600 Hz, and at a long range of up to 600 m.

Table 1. *Terrestrial laser scanner specification (Trimble SX12)*

SPECIFICATION	PARAMETER
ACCURACY	2 mm + 1.5 ppm
SCAN RANGE	600m
SCAN RATE	26,600 Hz
SCAN RESOLUTION	8.1 megapixels
FIELD OF VIEW	360° x 300°
FRAME RATE	15 fps

Laser scanned data were collected from the TLS instrument, as it provides a point cloud for estimating the tree dimensions and for post-processing. For the software, Computree, CloudCompare, and R-script were used for this project. Computree was used for data processing and generating QSM, CloudCompare for visualization and crown diameter extraction, R-script (ITSMe package) to obtain DBH, and tree height, and R-script for statistical analysis.

The basic wood density was obtained from Dryad website (https://datadryad.org/stash/dataset/doi:10.5061/dryad.234), a global wood density database that provides access to every tree species (Chave et al., 2009). Wood density is usually measured in g/cm^3 and refers to the mass wood per unit volume (table 2). The wood density varies among aspen and birch species, depending on growth condition, age, and wood structures. Therefore, higher value indicates denser wood, while lower value indicates less dense wood.

Table 2. *Basic wood density for aspen and birch trees*

TREE SPECIES	DENSITY (G/CM^3)
ASPEN (POPULUS TREMULA)	0.387
BIRCH (BETULA PENDULA)	0.525

3.3 Field measurement

3.3.1 Terrestrial laser scanning

A field measurement was carried out at in the study area on 18 April 2023, during early spring when the trees were in a leaf-off condition. This allows for a better visibility of the tree structure, allowing for detailed collection of point cloud data of branches, and other structural tree components. The weather condition on that day was sunny, windy and cold. The terrestrial laser scanning was conducted using Trimble SX12, in which the measurements were taken to obtain highly detailed and accurate point cloud data of different tree species for extracting tree attributes, such as DBH, tree height, and crown area. Multiple scan positions were set up around each tree to cover the entire tree canopy (figure 3). However, before taking these measurements, a station set up was carried out using the resection with three reference objects. Therefore, the instrument location at each scan position can be determined by measuring the distance and angles between the instrument and the reference objects.

Subsequently, seven scan positions were conducted to ensure the entire tree coverage using two different scan modes with a low-resolution setting to reduce the scan processing time. The first scan mode used the full dome to capture a 360-degree view, which is suitable for the two center positions. The second scan mode used the half dome, which covers half of the 360-degree view and was utilized for the corners of each scan position. Furthermore, to avoid collecting unwanted point cloud data outside of the tree plots, the total distance measurement was set to 30 meters. After collecting the point cloud data, which was consisted of about 27 million points, the data were then exported to the LAS file format and processed using the Computree software with the SimpleForest tool.

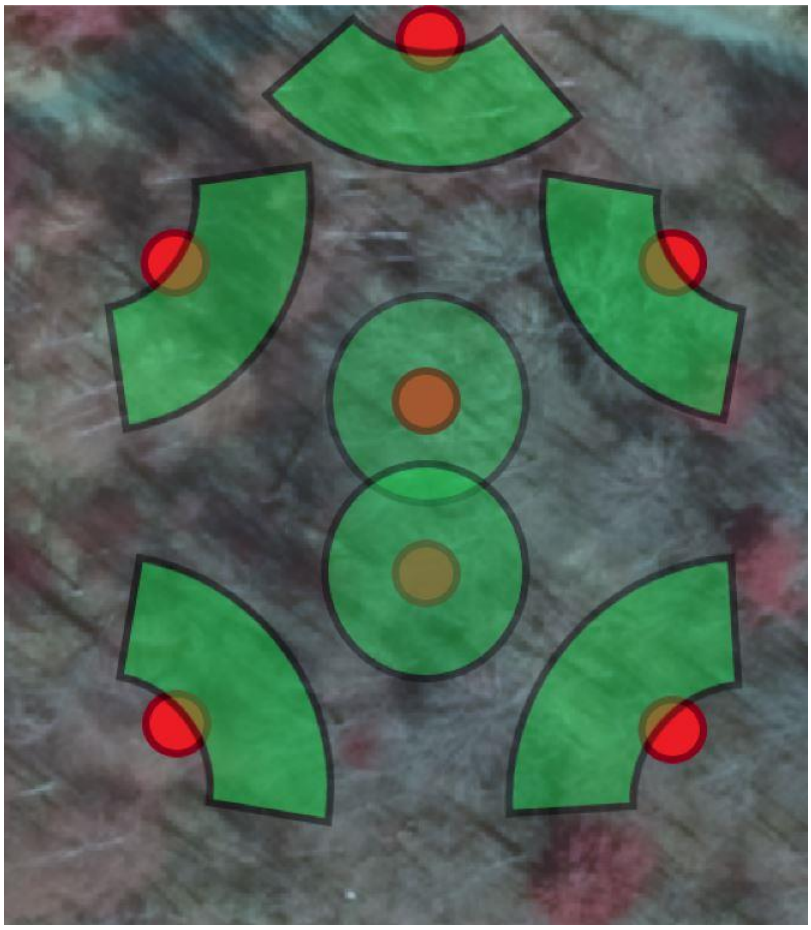

Figure 3. Scan positions of a forest using TLS in Valls Hage. Red circles represent scan positions. Green shapes represent full-dome and half-dome

3.3.2 Deriving validation data measurements

The validation data were collected and measured on 4 May 2023 using traditional field measurement methods and Trimble SX12. The weather condition was similar to the first field measurements. In the first one, a tape measure was used to get the DBH of each tree at 1.3 m height above the ground, which was then wrapped around the tree trunk to collect the values (figure 4, middle). Afterwards, Trimble SX 12 was used to measure the height of each selected tree. To achieve this, the instrument was oriented towards the tree, and the tree height was taken by sighting the instrument at the base of the tree, and then at the top of the tree (figure 4, left). The tree height was calculated using trigonometry, by measuring the horizontal and slope distances between the base and the top. This involved multiplying the horizontal distance by the tangent of the vertical angle, from the base to the top of the tree, to acquire the height information. Lastly, the crown diameter was determined, using a tape measure, by measuring the widest and the narrowest point of the crown, from both vertical and horizontal angles (figure 4, right). To obtain the crown diameter, the sum of the widest and narrowest distance was calculated, and then divided by two. The procedure was performed for all ten trees (five for aspen and five for birch).

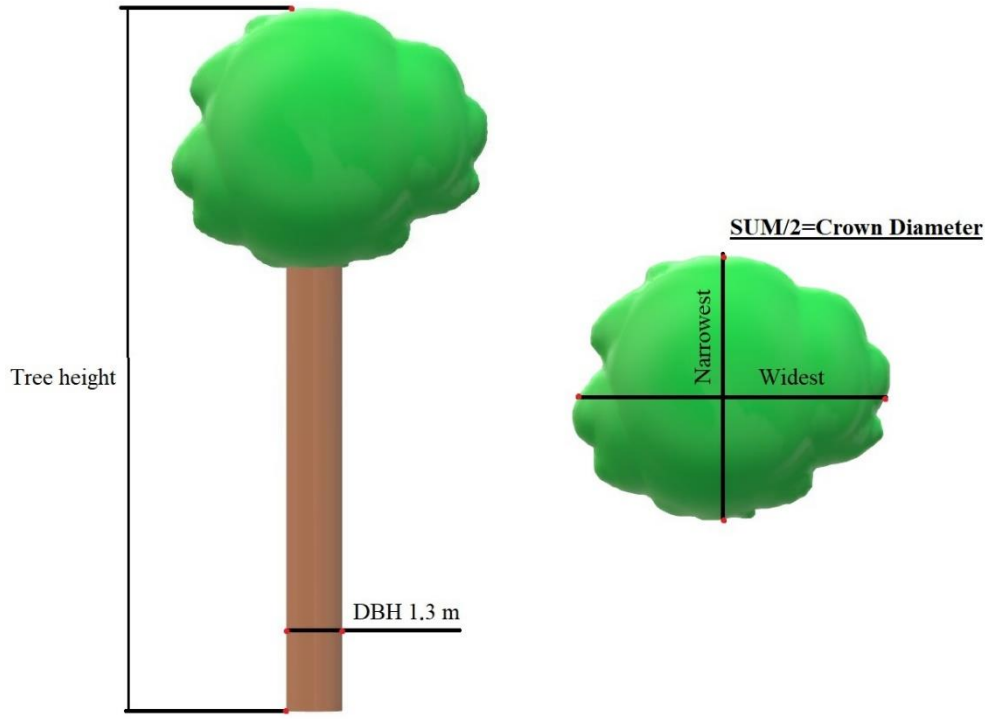

Figure 4. DBH, tree height and crown diameter measurement (left tree height and DBH) (right crown diameter)

3.4 Data processing

After collecting the LiDAR data, the following data processing steps were performed: merging multiple LAS files and exporting to XYB file format (.xyb), as the software Computree only supports this specific format. Then, filtering and segmentation were performed to identify individual trees and remove any noise or unwanted data. Subsequently, DBH and tree height were automatically extracted using R-script (ITSMe) software, and crown diameter using digital tape measurement in CloudCompare software. Finally, a QSM was generated to acquire the volume of each tree for estimating the biomass in the final step. These steps will be explained in further detail in the following subsections.

3.4.1 Merging LAS files

Before filtering and the segmentation of the LiDAR data could be performed, it was necessary to merge several LAS files. The merging step was done using Simpleforest tool in the Computree software, and the resulting file was exported in the XYB file format. Figure 5 illustrates the workflow involved in the merging and exporting process.

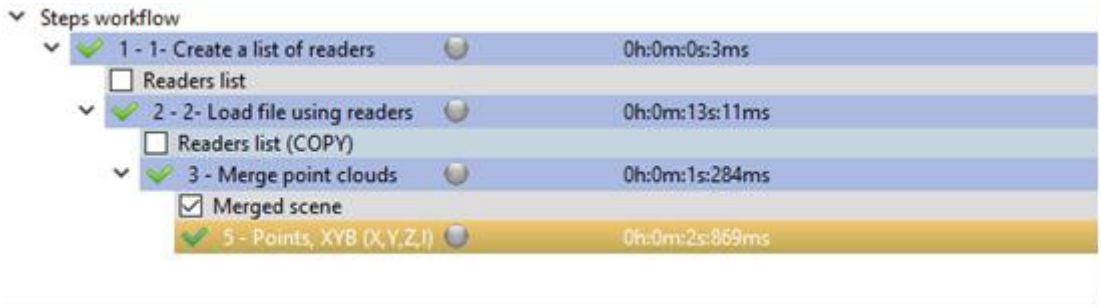

Figure 5. Merging LAS files

3.4.2 Filtering and segmentation

With the resulting merged file (figure 6), it was necessary to filter the noises, remove unwanted data, and to perform segmentation, to able to separate the ground points from vegetation points, along with being able to identify individual trees.

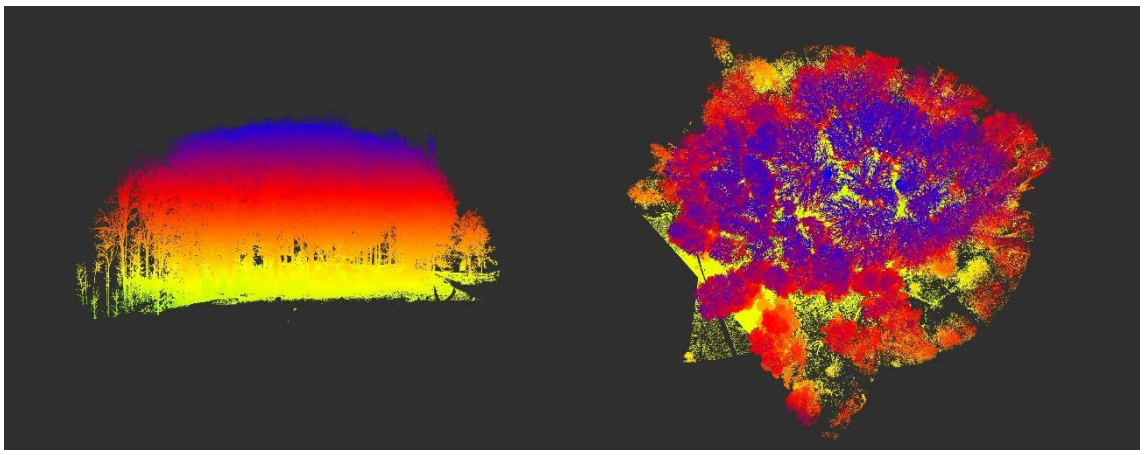

Figure 6. Merged LAS files with two different camera position: horizontal plane (left) and top plane (right)

The first major step in data processing involves the classification of point cloud data into ground points and vegetation points by creating a grid based on minimum elevation values and calculating point densities within specific elevation ranges (figure 7). The parameters for this classification were set to standard and not manually modified. This separation allows for the generation of digital terrain model (DTM) from the ground points, which is crucial for further analyses, and for it to be used as a reference surface.

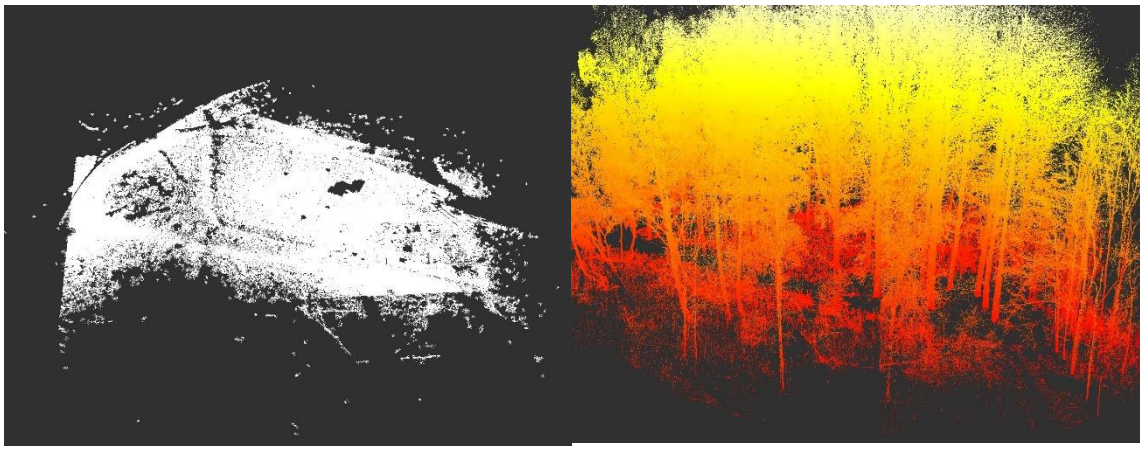

Figure 7. Separation of ground points (left) and vegetation points (right)

With the resulting ground points, the DTM was generated to help with the identification of ground points and to be able to remove non-ground objects, such as dead branches and small vegetation.

The next step was the segmentation of stems, and filtering of outliers and noises, which were relevant for the identification of individual trees. However, before the locations of the stems can be identified, delineation of the point cloud DTM was utilized to separate them into two parts, upper and lower, based on a specified threshold value. Therefore, the points with a certain threshold height were put into the lower point cloud DTM, while the remaining points above the threshold were put into the upper cloud. In this case, a 1.5 m threshold height above the DTM was used to be able to identify stems along with surrounding vegetation (figure 8, top left).

From there, the stem filter was utilized to separate the stem points from the noise points. The filtering was based on the angles between the point's growth direction and the z-axis, which resulted in to two different classes: stem points and noises. Standard parameters were used for the filtering, based on the software developer's recommendation. In addition, unwanted outlier noises were filtered out (figure 8, top right).

After separating the stem points from the noise points, the *Segmentation Euclidean Clustering* was performed to produce stem segmentation. In this step, the points were grouped into clusters based on a specified range of parameter, and clusters containing less than the specified number of points were removed (figure 8, bottom left). The parameters had to be carefully adjusted several times until the clusters of stems were individually grouped. In this case, a range of 0.1 m, and clusters containing minimum 1 of points were used.

Following the segmentation of individual stems, the *Dijkstra segmentation* was used to connect the segmented clusters to the upper clouds. In this process, the point cloud was first downscaled using the voxel grid to ease the connection, and then the tree ID of each segmented cluster searched for the neighboring upper cloud using Dijkstra's algorithm. This allowed the segmentation of the upper clouds, which was based on the segmented seed clusters (figure 8, bottom right). However, it was crucial to carefully choose the parameters, since the range of connectivity could unintentionally cluster points belonging

to neighboring trees. After the *Dijkstra segmentation*, the *Voronoi-based segmenta*tion was utilized to segment the remaining upper cloud.

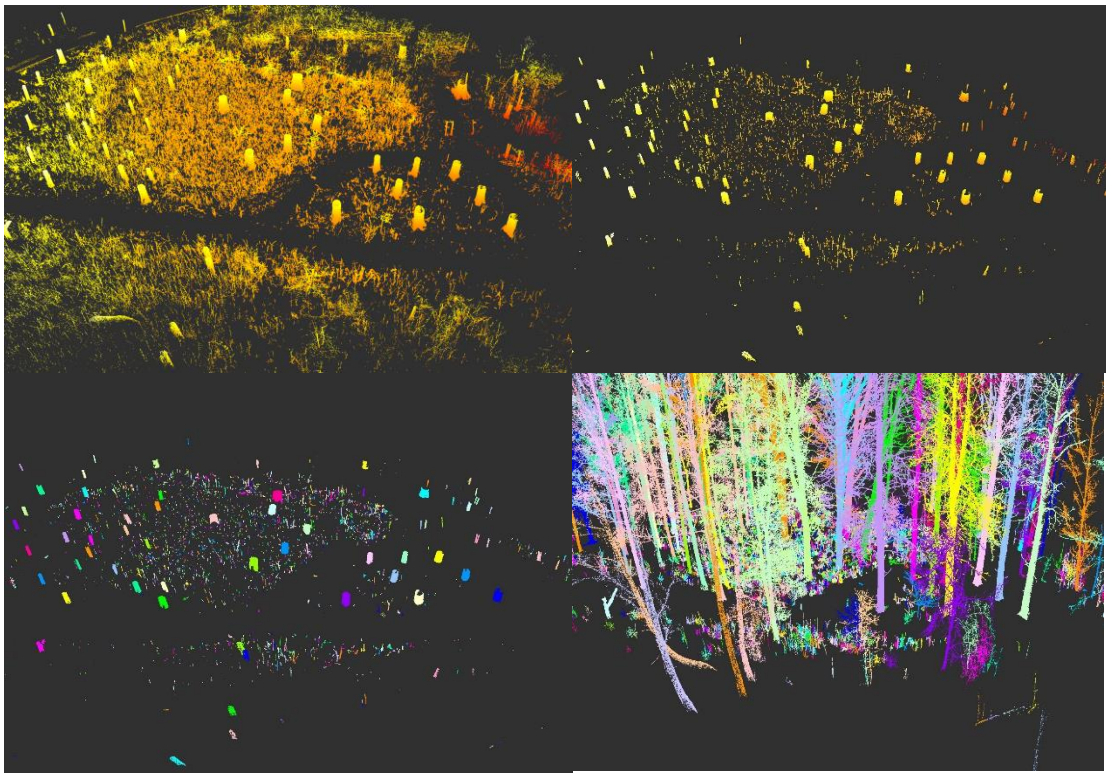

Figure 8. Top left shows the stems along with surrounding vegetation. Top right shows the stem filtering with separation from the surrounding vegetation. Bottom left shows the segmentation of individual stems. Bottom right shows the Dijkstra segmentation with connected stem and upper-cloud tree vegetation

With the segmented tree clouds, the remaining small vegetation clouds were removed to distinguish between undergrowth and trees using a height-based threshold, as shown in Figure 9. The algorithm's decision was based on the height of the segmented tree clouds, allowing the vegetation to be split into undergrowth and trees. The threshold was set to 8 m, wherein values below 8 m indicate undergrowth and values above indicate trees. This threshold was determined to focus on the analysis and estimation for larger, mature trees in the study area. Furthermore, any remaining poorly segmented trees with missing information were manually removed to improve the succeeding analysis for generating QSM.

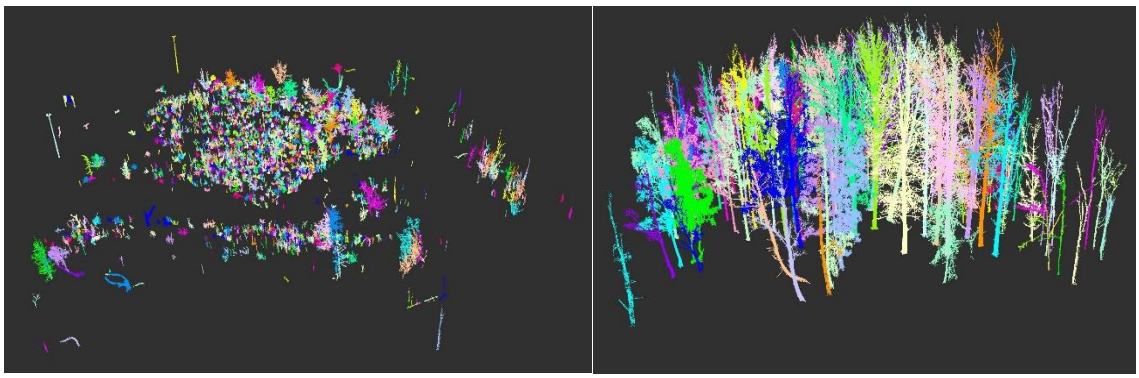

Figure 9. Filtered undergrowth vegetation with height < 8 m (left) and filtered trees with height > 8m (right)

3.4.3 Deriving tree attributes

Extracting tree attributes such as DBH and tree height was performed through R-script, using the ITSMe packages, together with the inputs from the segmented tree clouds for both birch and aspen tree derived in Section 3.4.2. The R-script were then utilized to obtain basic structural metrics from individual tree including the DBH and tree height.

Crown diameter was extracted from the segmented point cloud data using manual measurements in CloudCompare software, following a similar procedure as described in section 3.3.2 for the validation data. It is important to note that the manual measurements in CloudCompare was conducted for a total of ten trees, five for aspen and five for birch trees, which is similar to the number of trees measured in the field.

3.4.4 Generating QSM

Through the resulting segmented tree clouds in section 3.4.2, QSM was generated from several steps, and the aim was to fit QSM tree model to point cloud trees as close as possible. The first step was separating the two different tree groups, birch and aspen, into individual group, as they require different approach due to the specific characteristics and structures of the trees. The separation of the two different tree species, aspen and birch, were achieved through a manual assessment of their specific characteristics and structures. This also involved visually inspection of the trees on-site to accurately identify and classify them into individual groups.

Afterward, the *spherefollowing* tool was utilized to fit cylinders into a tree cloud and for constructing a tree model. Different fitting circle methods can result to different results, as shown in Figure 10. For aspen trees, the *Gauss Newton Least Squares* method was chosen due to its robust optimization algorithm, which aims to minimize the errors between the model and the point cloud data. For the birch tree, the *center of mass with median distance radius* was chosen, due to its irregular and branching structure. This method can provide a better result for birch trees due to its ability to handle the complexity of the tree. The rest of the parameters were set to standard - however, they can be adjusted if necessary to obtain the desired result.

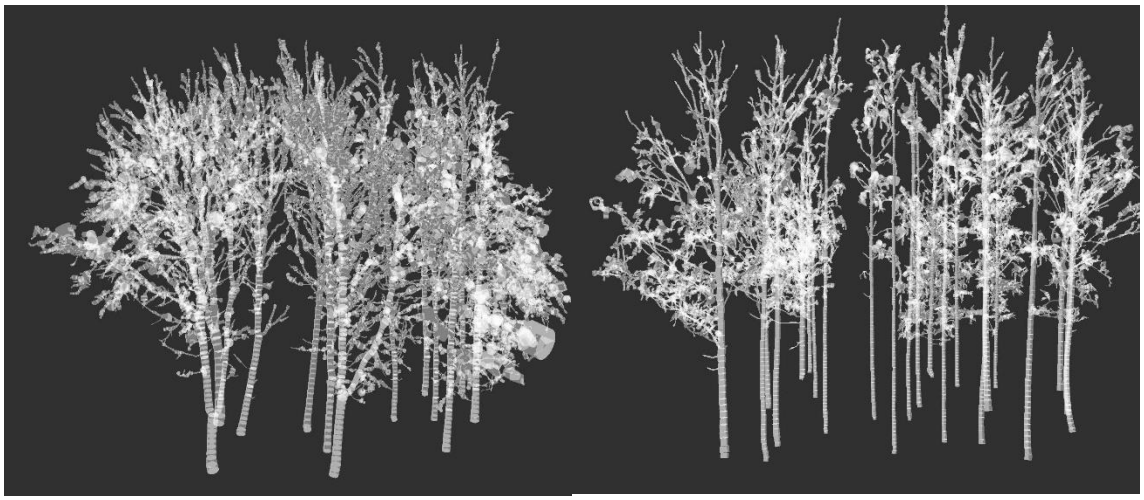

Figure 10. The first step in the QSM process for Aspen trees (left) and Birch trees (right)

As the first step of QSM, it needs further filtering to improve the cylinder structure and size (figure 11). This can be achieved from the second step by applying a *median filter tool* to adjust the median values of the surrounding cylinders, resulting in a more accurate QSM.

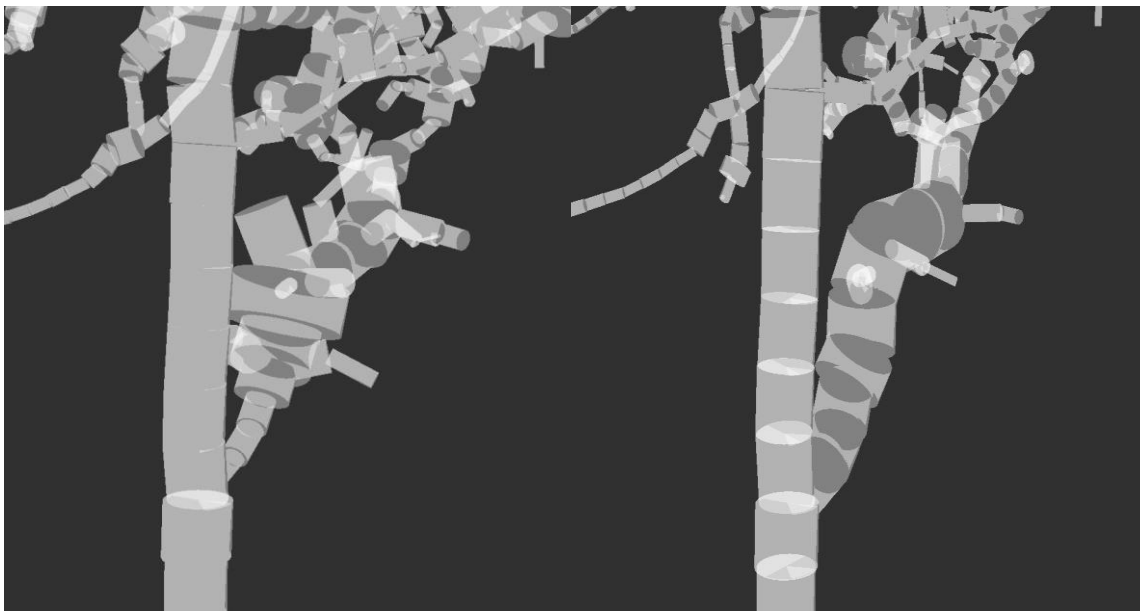

Figure 11. The unimproved (left) and the improved (right) QSM in close views (taken from birch tree as an example)

With the improved QSM, the third step was performed by utilizing *QSM Detect Wellfit Cylinders*, with the purpose to only estimate the best quality cylinders from the QSM model (figure 12). The inputs for this step were the results of the second step and the segmented point clouds, where the points were allocated to cylinders, resulting to each cylinder to be generated as a sub cloud. Meaning, the average distance of each sub cloud and corresponding cylinder was computed. The output was split into two parts of well- and bad fitted cylinders. Only the cylinders with a small enough average distance were considered well-fit, and cylinders that were close to the tips of the trees (twigs) with larger average distance were considered as bad fitted cylinders, due to higher errors.

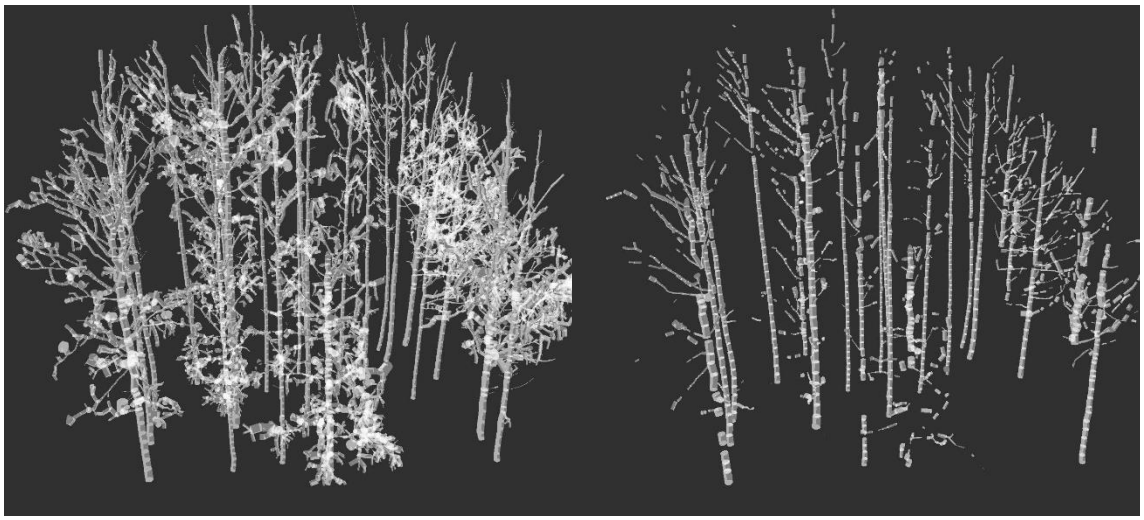

Figure 12. Undetected well-fitted cylinder (left) and detected well-fitted cylinder (right) (taken from birch trees as an example)

Lastly, using the well-fitted cylinders, the final step was performed to correct under or overestimated values in the QSM to improve its accuracy. In the *allometric correction*, an algorithm was used to detect incorrectly fitted cylinders, which have to be corrected. After experimenting with different parameters for the QSM model, the chosen parameter for birch trees was *taper correction*, and *vessel volume* for aspen trees. *Taper correction* is represented more accurately from the tree stems, since tree stems decrease in diameter as they extend from the base to the top. However, for the aspen trees, two of ten QSM had to be adjusted manually due to underestimated cylinders of branches, and prior to using *vessel volume*. *Vessel volume* is more robust and reliable for estimating cylinder volume by reducing the impact of twig radius errors. Finally, both aspen and birch QSM trees were exported to various formats, such as text (.txt) and 3D-files, which can be used for statistical analysis and estimating biomass. In addition, the volume was extracted from the exported QSM file.

3.5 Validation and statistical analyses

Derived volume from exported QSM can be utilized to estimate AGB along with wood density, as used in the current study. This was achieved by multiplying the volume derived from QSM with the specific wood density (equation 1) value obtained from Table 2. The accuracy of the volume data was visually assessed by observing the difference between the QSM and point cloud data. Therefore, no uncertainty values were calculated in this study.

$$AGB_{QSM} = QSM\ volume \times Wood\ density \quad (1)$$

Another AGB estimation was conducted using the allometric equation obtained from GlobAllomTree (GlobAllomeTree, n.d.), an international web platform that provide access to tree allometric equations. The tree-specific equation used for aspen (equation 2) and birch (equation 3) was given by (Johansson, (1999a, 1999b), and is purely based on DBH measurement, along with the coefficients.

$$AGB_{DBH,\ aspen} = 0.00146 \times (DBH)^{2.603533} \quad (2)$$

$$AGB_{DBH,\ birch} = 0.00029 \times (DBH)^{2.50038} \quad (3)$$

The comparison of different tree attributes, including DBH, height and crown, derived from both TLS data and validation data, was conducted using linear regression analysis with respect to 1:1 line to determine the accuracy. RMSE measures the overall error between predicted (TLS) and actual (validation) values with the following formula (equation 4):

$$RMSE = \sqrt{\sum_{i=1}^{n} \frac{(\hat{yi} - yi)^2}{n}} \quad (4)$$

where, $\hat{yi}$ represents predicted value, yi is the actual value, and n is the number of observations.

Afterwards, the AGB values obtained from both TLS data and validation data were compared using multiple statistical analyses, including RMSE, Coefficient of Variation (CV) RMSE, and Concordance Correlation Coefficient (CCC). CV (RMSE) measures the mean variable of the error between predicted (validation) and actual (TLS) values with the given formula (equation 5):

$$CV\ (RMSE)\ = \frac{RMSE}{\bar{y}} \times 100 \quad (5)$$

where the RMSE is divided by the mean of the actual values ($\bar{y}$) from validation AGB, and multiplying it by 100 to express it as percentage. This gives an indication of how close the predicted values are to the actual values. Meaning, a lower CV(RMSE) represent a more accurate model.

CCC, introduced by Lin (1989), measures the agreement between predicted (TLS) and actual (validation) values with ranges between 1 (perfect agreement) and -1 (bad agreement) with the following formula (equation 6):

$$CCC\ = \frac{2\rho\sigma_1\sigma_2}{\sigma_1^2+\sigma_2^2+(\mu_1-\mu_2)^2} \quad (6)$$

In the equation, ρ represents the Pearson correlation coefficient, σ_1 and σ_2 is the standard deviations of the predicted and actual values, and μ_1 and μ_2 correspond to the means of the predicted and actual values.

4. Results

A total of 32 trees were segmented and generated, consisting of 12 aspen trees and 22 birch trees. The remaining segmented point clouds, such as faulty vegetation, missing certain points, and objects outside of the plots were removed manually. Additionally, ten trees, consisting of five aspen and five birch, were selected, and measured separately for validation purpose.

The results are presented into four subsections. The first subsection focuses on the results of the segmented tree cloud for analyzing pre-processing and post-processing phases. The second subsection introduces the analyses of the extracted tree attributes for both aspen and birch trees, including DBH, tree height, and crown diameter. The third subsection presents the result of generated QSM for evaluating the model for aspen and birch trees. The last subsection focuses on the statistical analyses with linear regression, including RMSE, CV (RMSE), and CCC, from comparison of tree attributes and AGB values.

4.1 Segmented Tree Cloud

The result of segmented tree cloud after undertaking several steps of processing data in SimpleForest tool are shown in Figures 13 and 14. The left side represents pre-processing stage, while the right side illustrates the post-processing stage. The segmentation process identified and separated individual trees within the point cloud. Although some trees remain unidentified, or mistakenly clustered during segmentation, they can be manually removed while preserving other trees for generating QSM or undergoing further analyses to extract tree attributes such as DBH, height, crown diameter.

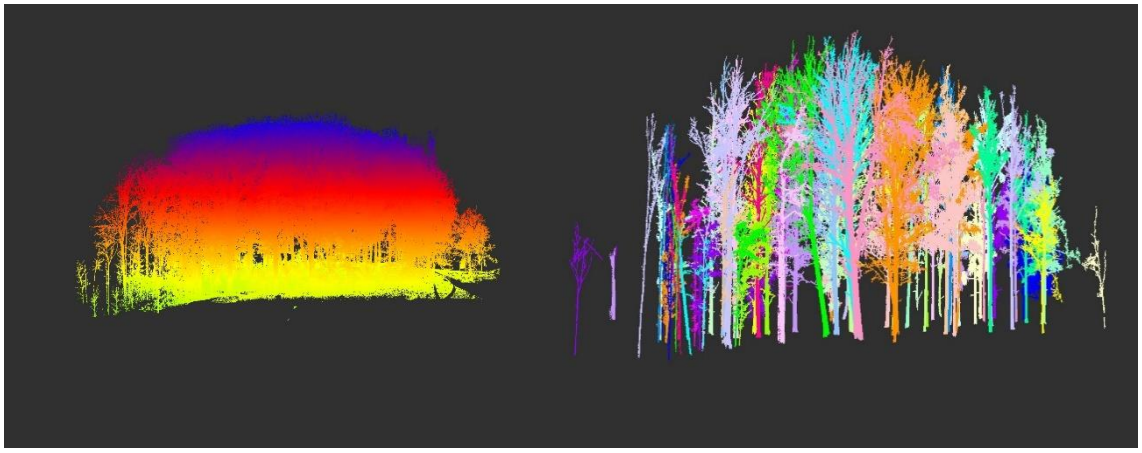

Figure 13. Results of segmented point clouds in horizontal views, before (left) and after (right) processing

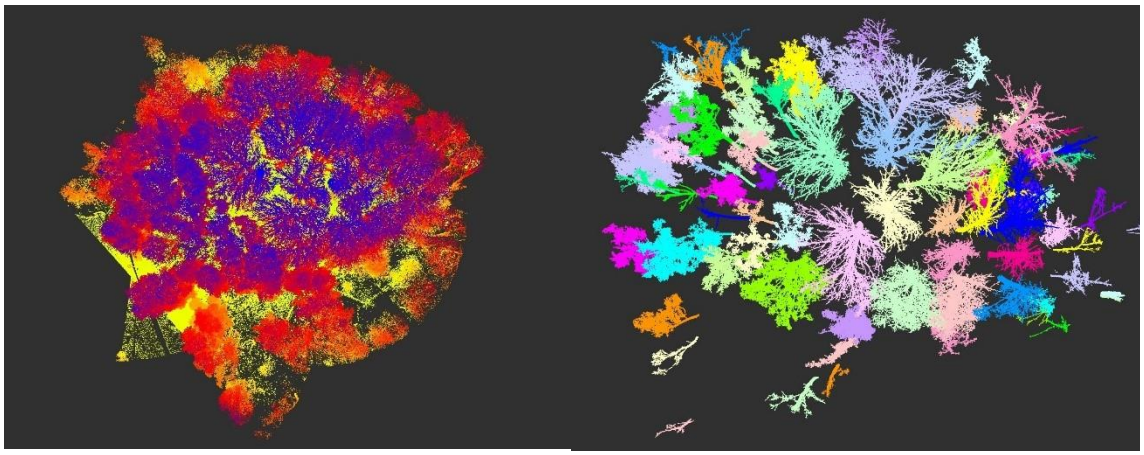

Figure 14. Results of segmented point clouds in top views, before (left) and after (right) processing

4.2 Extracted tree attributes

The results are represented using two illustrated models of individual tree species, aspen (figure 15) and birch (figure 16), along with the derived information of tree height and DBH. The left side indicate a tree height of 28.74 m for aspen, and 20.35 m for birch. On the right side, the DBH are displayed in two different manners. The first one is the DBH acquired from concave hull, with a value of 0.88 m for aspen and 0.45 m for birch. The concave hull DBH follows the shape and pattern from the point stem slice.

The second one is the functional DBH (fDBH) used to determine the area of the concave hull which is given as a fitted circle. fDBH are measured with values of 0.89 m for aspen and 0.45m for birch, potential to provide better accuracy. Lastly, the residual of DBH (R2) indicates the overall residuals between DBH and fDBH with a value of 0.03 cm for aspen and 0 cm for birch. This suggests that the residuals between them are insignificant.

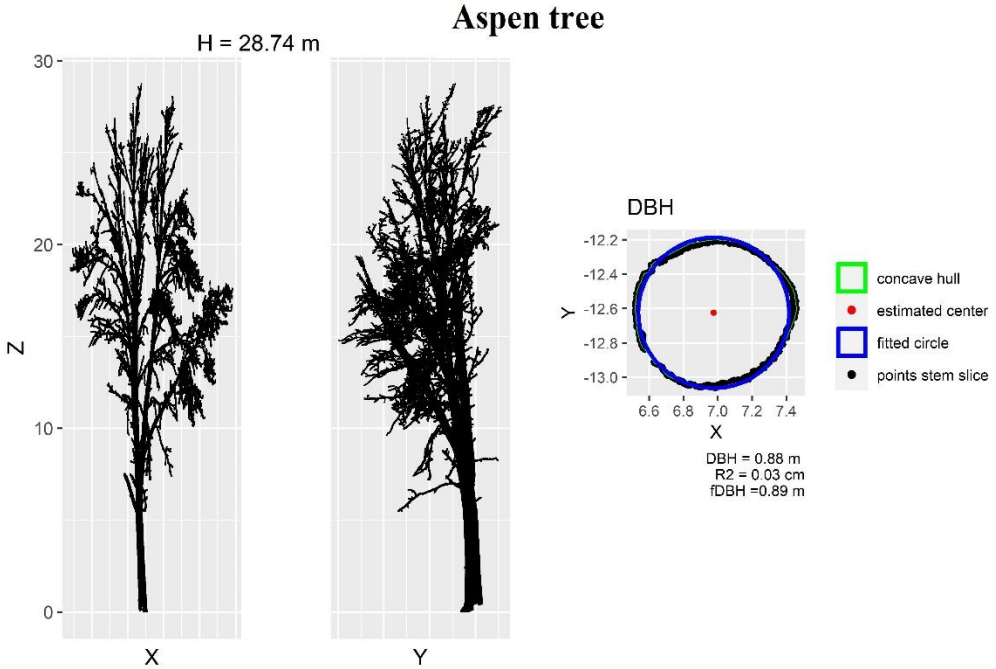

Figure 15. Result of single extracted aspen tree attributes. Tree height (left) and DBH (right)

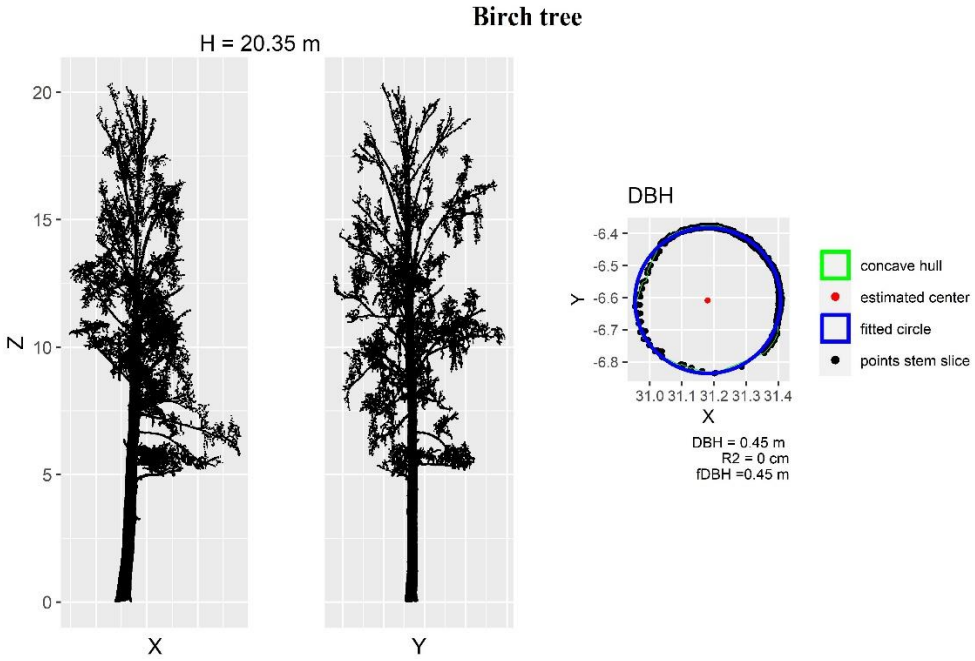

Figure 16 Result of single extracted birch tree attributes. Tree height (left) and DBH (right)

The extracted DBH, fDBH and the overall differences (R2) for each individual aspen trees are presented in Table 3. The table indicates that the largest available DBH is approximately 88 cm, compared to the fDBH of 89 cm, while the smallest value is around 46 cm for both DBH and fDBH. The largest overall residual between DBH and fDBH is 0.05 cm, while the smallest difference is 0.01 cm, indicating very small differences.

Table 3. *Results of extracted DBH for all aspen trees (cm), using DBH from concave hull and functional DBH (fDBH), together with their residuals (R2).*

ASPEN ID	DBH	FDBH	R2
ASP_1	87.75	89.24	0.03
ASP_2	73.92	74.76	0.03
ASP_3	72.46	70.49	0.05
ASP_4	58.82	58.67	0.01
ASP_5	65.08	64.17	0.04
ASP_6	59.70	60.73	0.02
ASP_7	62.19	64.00	0.03
ASP_8	58.81	60.44	0.02
ASP_9	46.49	46.79	0.02
ASP_10	48.94	49.43	0.01
ASP_11	57.60	58.36	0.01
ASP_12	53.33	49.51	0.02

Similar observations are presented for each individual birch trees (table 4), indicating that the largest DBH and fDBH is approximately 45 cm, while the smallest measurement for both DBH and fDBH is around 24 cm. The residuals between DBH and fDBH range from 0 to 0.01 cm, suggesting insignificant differences.

Table 4. *Results of extracted DBH for all birch trees (cm), using DBH from concave hull and functional DBH (fDBH), together with their residuals (R2).*

BIRCH ID	DBH	FDBH	R2
BIRCH_1	45.4	45.3	0
BIRCH_2	36.5	36.9	0.01
BIRCH_3	50	50.3	0.01
BIRCH_4	42.7	42.8	0.02
BIRCH_5	26.6	26.1	0
BIRCH_6	36.2	36	0
BIRCH_7	44.7	45.2	0.01
BIRCH_8	32.3	32.8	0
BIRCH_9	32.6	32.3	0
BIRCH_10	38.8	39.6	0
BIRCH_11	37.1	37.8	0.01
BIRCH_12	39.1	39.8	0
BIRCH_13	31.9	32.4	0
BIRCH_14	33.7	34.6	0
BIRCH_15	27.2	27.4	0
BIRCH_16	33.8	28.8	0
BIRCH_17	27.2	27.6	0.01
BIRCH_18	24.4	23.9	0
BIRCH_19	23.7	24.1	0
BIRCH_20	30	30.3	0
BIRCH_21	29.6	30	0
BIRCH_22	27.3	27.2	0

The extracted tree heights of all individual aspen and birch trees are presented in Table 5. The highest height is approximately 27.7m for birch, and around 30.7 for aspen. On the other hand, the lowest tree height for birch measurements is around 19 m, and 27m for aspen.

Table 6 provides the information of extracted crown diameters from TLS and field validation for five individual birch trees. The largest crown diameter obtained from TLS is around 11 m, compared to the validation measurement of 12 m. On the other hand, the smallest measurement is approximately 3.5 m for TLS, while the validation measurement records 5 m. The differences between derived TLS and field validation crown data ranged from 0.4 to 1.9 m. These variations indicate noticeable differences for certain trees.

Table 5. *Result of extracted tree heights for aspen and birch trees (m)*

BIRCH ID	TREE HEIGHT	BIRCH ID	TREE HEIGHT	ASPEN ID	TREE HEIGHT
BIRCH_1	20.35	BIRCH_13	23.41	ASP_1	28.74
BIRCH_2	19.92	BIRCH_14	23.81	ASP_2	28.50
BIRCH_3	26.64	BIRCH_15	22.99	ASP_3	27.69
BIRCH_4	21.79	BIRCH_16	27.81	ASP_4	29.67
BIRCH_5	21.95	BIRCH_17	22.52	ASP_5	29.19
BIRCH_6	20.26	BIRCH_18	24.72	ASP_6	27.40
BIRCH_7	24.35	BIRCH_19	19.11	ASP_7	29.95
BIRCH_8	25.73	BIRCH_20	25.87	ASP_8	30.66
BIRCH_9	25.02	BIRCH_21	22.23	ASP_9	29.77
BIRCH_10	23.91	BIRCH_22	23.81	ASP_10	28.61
BIRCH_11	26.55			ASP_11	28.66
BIRCH_12	25.02			ASP_12	27.72

Table 6. *Result of extracted crown diameter for five birch trees (m)*

BIRCH ID	TLS CROWN	VALIDATION CROWN	DIFFERENCES
BIRCH_3	10.975	11.95	0.98
BIRCH_8	7.05	7.45	0.4
BIRCH_9	5.6	7.5	1.9
BIRCH_16	5.1	6.1	1
BIRCH_18	3.45	4.9	1.45

Similar observation for the five individual aspen trees is introduced in Table 7. The finding suggests that the largest crown diameter derived from TLS is approximately 15.5m, which is in consistent with the validation measurements of 15.5m. Following by the smallest measurement is around 6.5m for TLS, and 7.2m for validation. The differences between TLS and validation for crown diameter is 0 to 0.7m, indicating average differences.

Table 7. *Result of extracted crown diameter for five aspen trees (m)*

ASPEN ID	TLS CROWN	VALIDATION CROWN	DIFFERENCES
ASP_1	15.5	15.5	0
ASP_5	8.68	8.3	0.38
ASP_4	9.55	9.85	0.3
ASP_6	10.3	10.75	0.45
ASP_9	6.5	7.2	0.7

4.3 Quantitative structure models for aspen and birch

The QSMs for the birch tree were generated and are introduced in three different visualizations (figure 17). The left side displays the segmented point cloud of individual tree. In the middle, the generated QSM is illustrated with different color based on the amount of volume. The right side of the figure displays the combination of segmented tree cloud and the QSM, discovering the differences.

Birch trees typically have irregular and more complex structures, consisted of numerous smaller twigs and noises. Regardless of the challenges, the QSM for the birch tree still captured its complex characteristics by utilizing *taper correction* to minimize the error between point cloud and QSM.

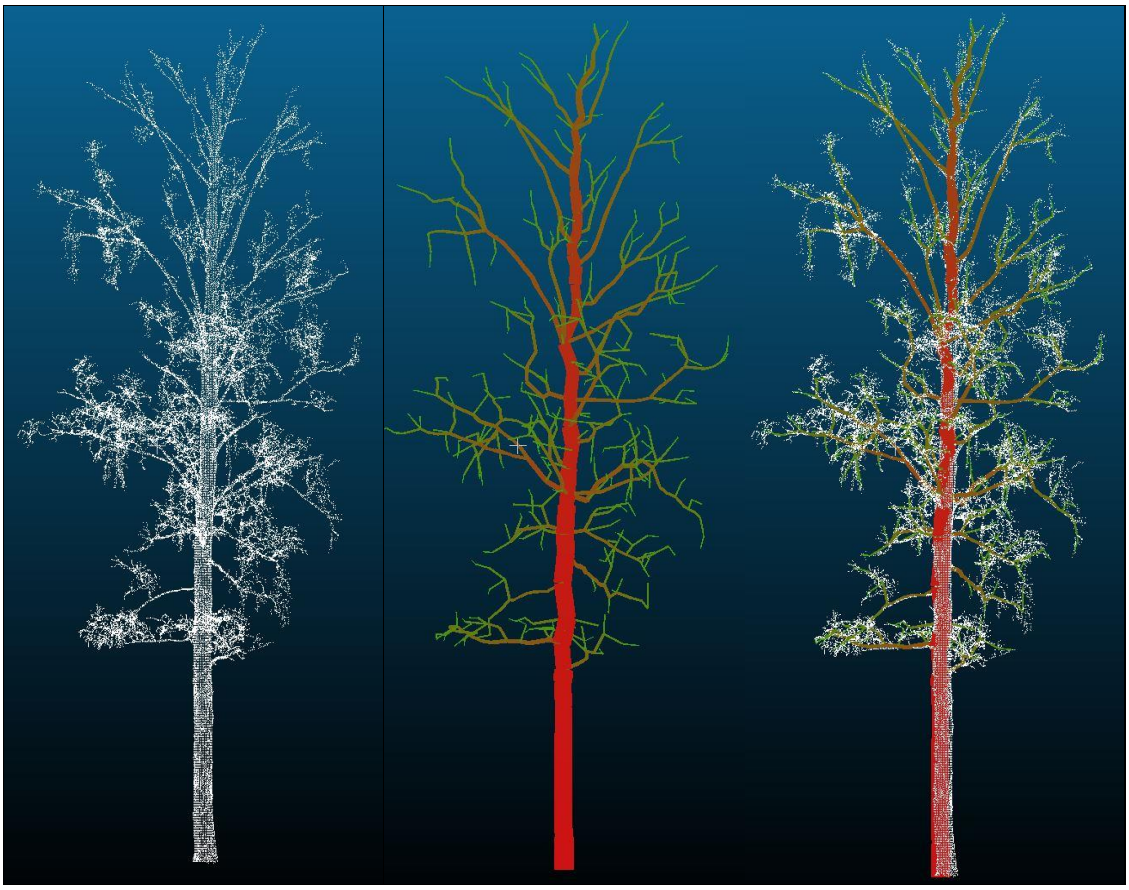

Figure 17. The results show three different models of a single birch tree, where the left shows point cloud, middle QSM and right combined

The generated QSMs for aspen (figure 18) are presented in similar manner as the visualization for birch trees Aspen trees generally have more regular and patterned structure compared to birch trees, with lesser twigs and lesser complexity. This type of characteristics allows the utilization of vessel volume, from point cloud to the QSM, to effectively capture the structure and pattern for aspen trees.

While vessel volume method generally captured the aspen tree structure better, some branches may had been underestimated in size of cylinders in the QSM. This can be observed in the combination of segmented tree cloud and the QSM on the middle and

right-side (figure 18). In that instance, certain branches that should be classified as medium or large appeared smaller than intended in the QSM. Nevertheless, the resulting QSM still provided a reliable representation of the aspen tree's structure and can be used to estimate the volume.

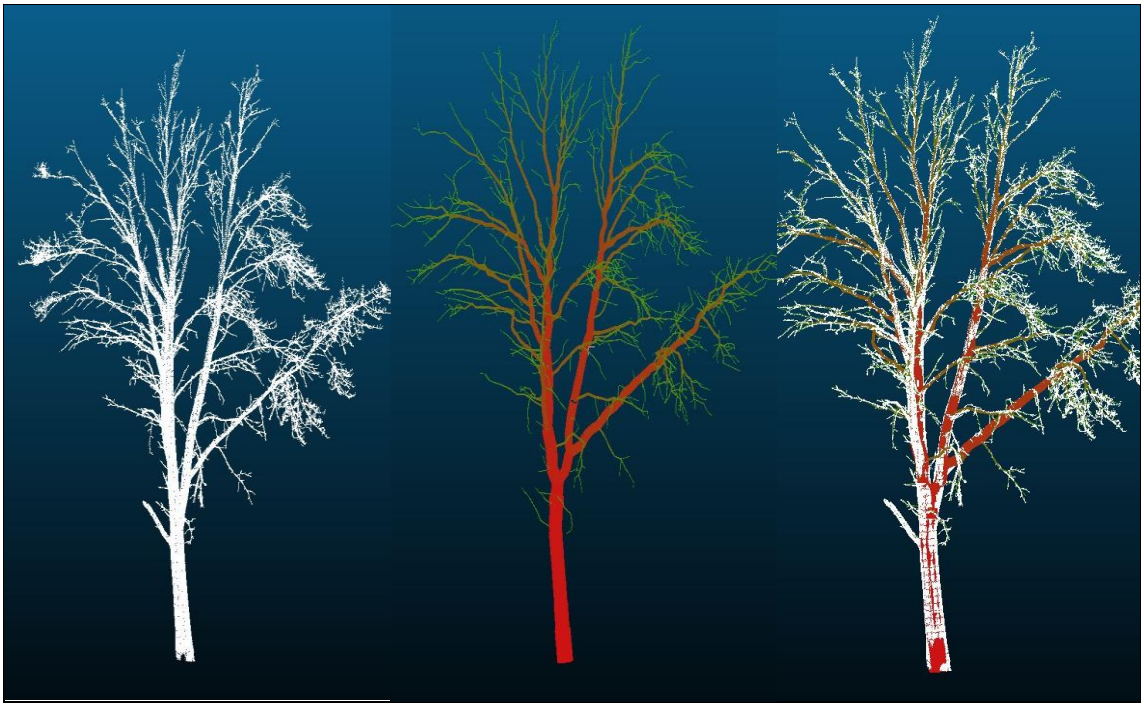

Figure 18. The results show three different models of a single aspen tree, where the left shows point cloud, middle QSM and right combined

The generation of QSMs for both aspen and birch was visualized using CloudCompare software (figure 19). The figure displays a comprehensive representation of the tree structure, capturing the whole characteristics of both tree groups. The results from the QSMs, give the possibility to analyze the details of the tree structure, including thickness, angles and overall form of branches, allowing it to be used for further analysis and for comparison between among tree species or groups.

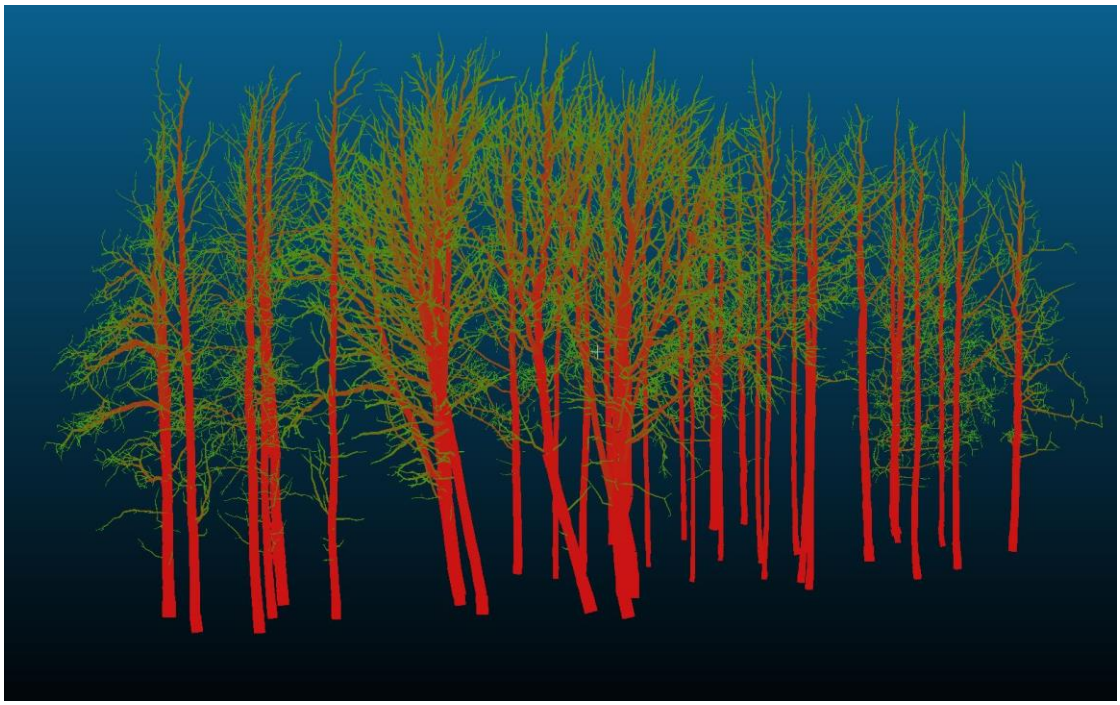

Figure 19. The results show 3D-cylinder model of whole trees in Cloud Compare software

4.4 Tree volumes from QSM

Volume estimates were also derived from QSMs for both aspen (table 8) and birch (table 9) trees. These tables represent the total volume of every tree, and are expressed in cubic meters (m^3). The largest volume derived for the aspen trees is approximately 17 m^3, while the smallest measurement is around 3 m^3. On the other hand, for the birch trees, the largest volume is around 3 m^3, followed by the smallest measurements of approximately 0.5 m^3. These estimated volumes provided essential information for AGB estimation.

Table 8. *Result of derived volume for all aspen trees (m^3).*

ASPEN ID	VOLUME
ASP_1	17.09
ASP_2	10.48
ASP_3	8.79
ASP_4	6.55
ASP_5	7.86
ASP_6	6.34
ASP_7	7.72
ASP_8	6.03
ASP_9	3.74
ASP_10	3.28
ASP_11	4.72
ASP_12	4.80

Table 9. *Result of derived volume for all birch trees (m^3)*

BIRCH ID	VOLUME
BIRCH_1	2.62
BIRCH_2	2.24
BIRCH_3	3.22
BIRCH_4	1.96
BIRCH_5	0.83
BIRCH_6	1.26
BIRCH_7	2.43
BIRCH_8	1.19
BIRCH_9	1.19
BIRCH_10	2.01
BIRCH_11	1.59
BIRCH_12	1.28
BIRCH_13	1.14
BIRCH_14	1.33
BIRCH_15	0.75
BIRCH_16	1.44
BIRCH_17	0.79
BIRCH_18	0.55
BIRCH_19	0.66
BIRCH_20	0.89
BIRCH_21	0.94
BIRCH_22	0.75

4.5 Validation

4.5.1 Comparison of Tree Attributes

The comparison between field validation measurement and TLS was conducted using R-script. The left side of Figure 20 illustrates the comparison for DBH of aspen and birch. The linear regression indicates an RMSE of 1.33 cm. With observing the predicted and actual values, they can be concluded that most values were slightly underestimated.

The comparison for tree height of aspen and birch trees are displayed in Figure 19 (right) The linear regression shows an RMSE of 1.05 m, which indicates a noticeable error between the predicted and actual values for each point.

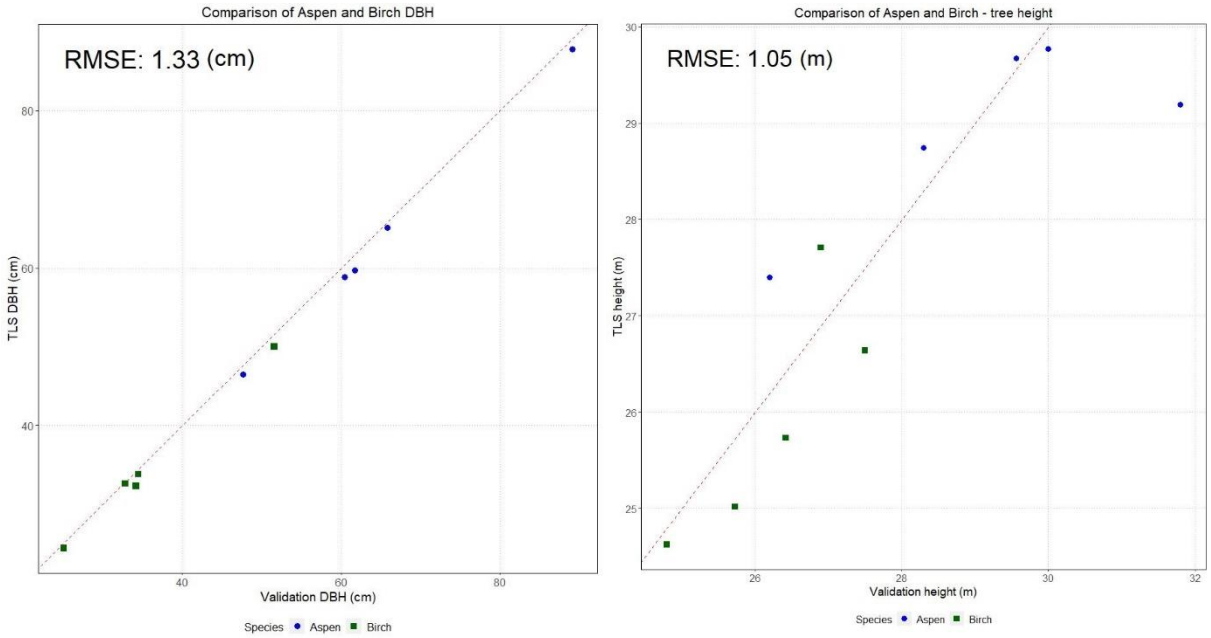

Figure 20. Results of comparison from both aspen and birch trees using TLS data and validation data (left, DBH; and right, tree height)

When comparing the TLS derived and manually measured crown diameters of aspen and birch trees (figure 21), the linear regression analysis has an RMSE of 0.94 m. Most of the aspen trees show a slight underestimation of the crown diameter, except for one tree that is slightly overestimated. Additionally, one of the aspen trees with a crown diameter of more than 15 m is perfectly fitted to the regression line. However, for the birch trees, the increase in error for crown diameters is noticeable.

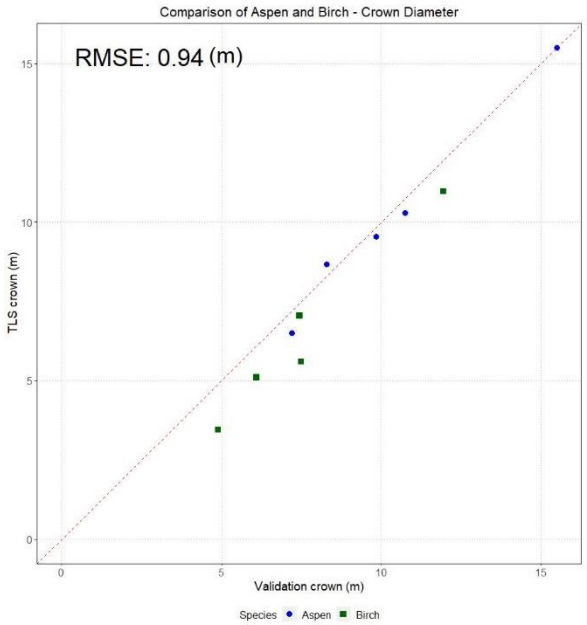

Figure 21. Result of comparison with crown diameter from both aspen and birch trees using TLS data and validation data

4.5.2 Above-ground biomass

AGB estimations and the differences for individual aspen trees are presented in Table 10. The table consists of TLS derived AGB from QSM equation (equation 1), as well as TLS- and field-based AGB validations using the DBH-based tree species equation (equations 2 and 3). Also shown in the table are the differences in the AGB computations by subtracting (i.e. the difference between TLS QSM and derived TLS DBH, and the difference between TLS QSM and field validation). However, it is worth noting that the field validation AGB includes only a total of ten validated trees, while the TLS data covers all trees.

The largest AGB estimation is approximately 6.600 kg for TLS QSM, 6700 kg for TLS validation, and 7000 kg for field validation. On the other hand, the smallest recorded AGB is around 1300 kg for TLS QSM, 1300 kg for TLS validation, and 1350 kg for field validation. The differences between TLS QSM and TLS validation range from -247 to 672 kg, while the differences between TLS QSM and field validation range from -72 to 375 kg. These results indicate noticeable differences for particular aspen trees.

Table 10. *Result of AGB estimation and differences for all aspen trees (kg)*

TREE TYPE	**AGB ESTIMATION**			**DIFFERENCES**	
ASPEN ID	TLS QSM (equation 1)	TLS validation (equation 2-3)	Field validation (equation 2-3)	TLS QSM - TLS validation	TLS QSM - Field validation
ASP_1	6615	6707	6990	92	375
ASP_2	4054	4295		241	
ASP_3	3400	4072		672	
ASP_4	2533	2369	2551	-165	18
ASP_5	3042	3087	3175	46	133
ASP_6	2454	2464	2685	10	231
ASP_7	2989	2742		-247	
ASP_8	2335	2369		33	
ASP_9	1446	1286	1374	-161	-72
ASP_10	1271	1474		203	
ASP_11	1828	2245		417	
ASP_12	1859	1834		-24	

A similar analysis is performed for birch trees (table 11). The largest estimated AGB is observed to be around 1700 kg for TLS QSM, 1625 kg for TLS validation, and 1760 kg for field validation. Subsequently, the smallest estimated AGB is approximately 300 kg for TLS AGB, 270 kg for TLS validation, and 290 for field validation. The differences between TLS QSM and TLS validation range from -437 to 209, while the differences between TLS QSM and field validation range from -111 to 68. These estimated AGB values indicate significant differences for certain birch trees.

Table 11. *Result of AGB estimation and differences for all birch trees (kg).*

TREE TYPE	AGB ESTIMATION			DIFFERENCES	
BIRCH ID	TLS QSM (equation 1)	TLS validation (equation 2-3)	Field validation (equation 2-3)	TLS QSM / TLS validation	TLS QSM / Field validation
BIRCH_1	1377	1277		-100	
BIRCH_2	1177	740		-437	
BIRCH_3	1691	1625	1758	-66	68
BIRCH_4	1029	1095		66	
BIRCH_5	434	335		-99	
BIRCH_6	663	725		62	
BIRCH_7	1274	1228		-46	
BIRCH_8	625	545	629	-80	3
BIRCH_9	625	558	566	-68	-59
BIRCH_10	1056	862		-194	
BIRCH_11	833	771		-63	
BIRCH_12	669	879		209	
BIRCH_13	598	528		-70	
BIRCH_14	699	606		-93	
BIRCH_15	395	355		-41	
BIRCH_16	754	610	643	-143	-111
BIRCH_17	417	355		-62	
BIRCH_18	290	270	290	-20	0
BIRCH_19	346	251		-94	
BIRCH_20	465	453		-12	
BIRCH_21	495	438		-57	
BIRCH_22	394	358		-36	

The comparison between the derived TLS QSM and the DBH-based field tree species equation are presented in the graph in Figure 22. In this comparison, the field validation refers to the validation of AGB estimates using field measurements and the DBH-based tree species equation (equation 2-3). The linear regression displays an RMSE of 154 kg, indicating the average mean differences between the predicted values (TLS) and actual values (validation). The overall CV(RMSE) is 7.677%, which represents the mean variable of the RMSE. The agreement between predicted value (TLS) and actual value (validation) represents a correlation coefficient of 0.997, indicating near-perfect agreement. However, by observing the plot of linear regression, the TLS AGB estimation for aspen trees is generally underestimated against the field AGB estimation, particularly for trees with larger DBH.

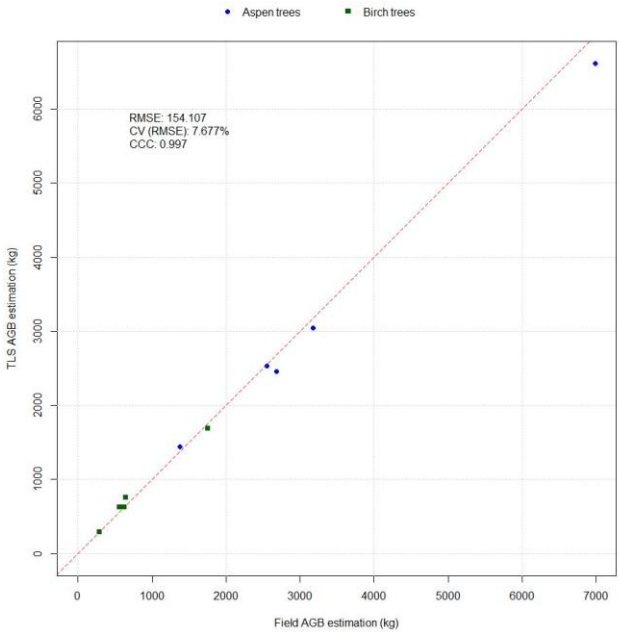

Figure 22. Result of AGB comparison between TLS QSM and field validation using R-script.

The results of AGB estimation from derived TLS QSM and TLS validation DBH based tree species equation from derived TLS model are also compared and presented (figure 23). The TLS validation refers to the validation of AGB estimates using TLS data and the same DBH-based tree species (equation 2-3). The linear regression indicates an RMSE of around 190 kg, which is higher than the previous figure. The overall CV(RMSE) is also higher with greater variability of a value of 18.881%. The CCC of 0.990 indicates a slightly lower, but still are considered as near-perfect agreement. The increase of RMSE and CV(RMSE) are not surprising, considering that the comparison is based on a total 32 trees, and that particular aspen and birch trees have noticeable differences in AGB.

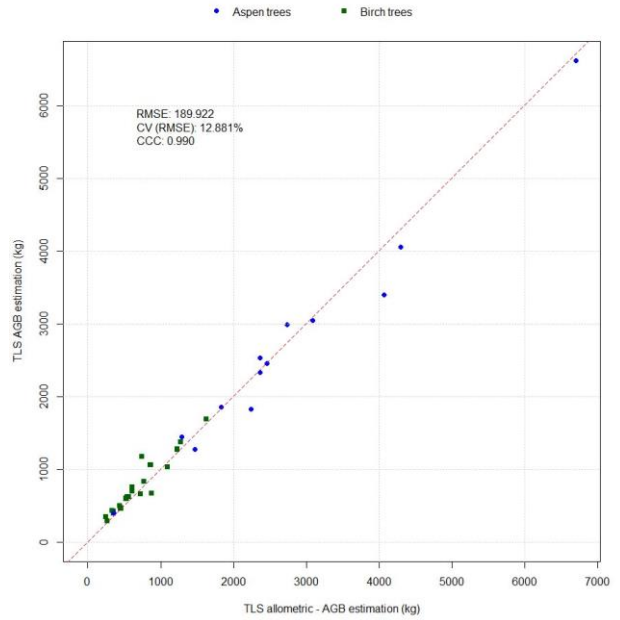

Figure 23. Result of AGB comparison between TLS QSM and TLS validation using R-script

5 Discussion

In the discussion, the first part discusses the difficulties and challenges encountered during the collection of validation data and the various phases of data processing. This involves the potential sources of error or selected parameters in the processing steps, which could impact the accuracy of the results using SimpleForest tool. Second part includes a discussion of the results, and explores the various factors that may influence the accuracy of the AGB estimates.

5.1 Approach

5.1.1 Validation data gathering

During the validation data gathering process in the field, tree attributes such as DBH, tree height and crown diameter were derived using a tape measure and the Trimble SX12 instrument. Using the tape measure for collecting the DBH provided to be straightforward and reliable both for validation purposes and the AGB estimations using allometric equations. However, challenges occurred during the measurements for the crown diameter and tree height.

For crown diameter measurements, the original idea was to utilize the Trimble SX12 to measure distance for crown diameter estimations. However, due to the overlapping canopies from the neighboring trees, it was difficult to measure from the ground. Therefore, an alternative option was to use traditional (manual) tape measurement to measure the crown diameter. This method is simple and effective, but can give less accurate estimations due to human bias when measuring from the ground. Thus, this can impact the results when comparing against TLS-derived data and for the AGB estimation using this tree attribute.

Regarding measurement of tree height, a single distance measure from Trimble SX12 was utilized. However, measuring tree height at top of the tree was also challenging, considering the overlapping canopies from the neighboring trees, and widely spread crowns. Furthermore, the wind condition made it more difficult due to the movement at top the tree that heavily affected the accuracy of measurements. This method appears to be unreliable and inaccurate for validation purposes. However, there are potential solutions for improving the accuracy of tree height measurements. The first one is ensuring the wind conditions are calm during the field measurements can minimize the movement of the top tree. The second one is adjusting the position of the instrument by moving farther away from the tree until the top of the tree is visible, to improve the accuracy of tree height measurement. Previous studies had shown similar difficulties with the field measurements of tree height (e.g. Calders et al., 2015). Calders et al. (2015) also utilized a single measurement of the top of the tree. The authors further argued that measuring the top of the tree from the ground is difficult due to the spread of crowns.

5.1.2 Tree reconstruction and modelling parameters

The ability to automatically segment and identify individual tree clouds and generate QSMs was successful. But certain processing steps had to be adjusted manually to achieve the desired result. The first challenge involved the *Segmentation Euclidean Clustering* step, which had to be re-adjusted multiple times to ensure that each stem was accurately segmented, and neighboring small vegetation was separated. This process can be time-consuming as every stem has different levels of characteristics and differences in point cloud density. Therefore, improving the possibility to remove neighboring small vegetation from each stem before the segmentation steps were conducted to contribute to a more accurate segmentation for individual stems.

The second challenge was the *Dijkstra segmentation* process, particularly the two primary parameters: the z-axis scaling factor between 0.1 and 1, and the connecting range to the neighboring upper point cloud of trees. These parameters were found to be sensitive to the output results. A too-small connecting range would not connect between the upper cloud tree and segmented cluster stems, while a too-long connecting range would unintentionally connect to the part of a neighboring tree.

When it comes to the z-axis parameter, the scaling input depends on the quality of the point, as a high scaling input increases the sensitivity to occlusion gaps. This can make the algorithm accidentally jump over to neighboring trees. Considering the average quality of the point cloud data used, and that neighboring trees were closely clustered to each other, the scaling input had to be set to low. This allowed the algorithm to overcome the occlusion gaps and to continue accurately segmenting the tree stems.

However, a few potential solutions can further be explored to reduce the need for manual adjustments in these parameters. The first one would be to increase the quality of point clouds during field scanning, although this will require more scanning processes. Secondly, the wind condition can affect the quality of point clouds, so ensuring the wind conditions, such as calm wind, would enhance the overall quality and accuracy of the point cloud data.

The third challenge involves the processing steps of the QSM using the *spherefollowing*. This step consists of several parameters that may be confusing for the beginner user (see appendix B). Jan et al. (2021), further emphasize that the parameters should be experimented with if the output result is not accurate with the default recommendation values. This is crucial, considering the nature of the different characteristics and structures of aspen and birch trees. Thus, adjusting these parameters and optimizing QSM processing can be time-consuming, as the processing time is dependent on the point cloud size and the complexity of the tree structure.

In general, the automated segmentation, filtering, identification of individual tree clouds, and generations of QSMs are considered reliable methods using SimpleForest tool. However, while the user guide provided by Jan et al. (2021) is helpful, there is still a potential for further improvement for a more comprehensive streamlined framework that

minimizes the need for manual adjustments of parameters. This could further reduce the overall time-consumed for data processing.

5.2 Findings

5.2.1 Accuracy of extracted tree attributes derived from TLS and validation

The results of the DBH comparison between TLS-derived and field validation data were consistent with each other, leaving only small differences (figure 20, left). This suggests that the DBH measurements acquired from TLS-derived data are accurate and reliable for both aspen and birch trees, which can be used in further analysis. However, it is important to consider the parameters used in the models and their impact on improving the results. In the study, R-script was used to extract tree information of individual tree models, offering two types of DBH computations.

The first type is the concave hull DBH, which effectively captures the shape and contour of the tree stem, providing precise DBH measurements. The second type is the fDBH, computed by determining the area of the concave hull derived from the point slice stem. The concave hull DBH from the models was chosen for comparison and estimating AGB using allometric equations, due to minimal overall differences observed (see tables 3 and 4).

However, a particular birch tree had missing point clouds on a certain side (appendix A), which contributed to a less accurate measurement of DBH from TLS. This can be addressed by ensuring that the TLS scan fully captures the entire tree from all sides or consider utilizing fDBH. By doing so, greater robust and reliable results for tree analyses can be done.

The RMSE differences between TLS-derived height and field validation height were noticeable (figure 20, right). The largest difference recorded for one particular aspen tree is approximately 2 m, which could be associated with uncertainty in the field measurements. In the study, Trimble SX12 was used for one single measurement at the base and top of each tree. These measurements can be challenging due to factors such as wind conditions, the large crowns, and clusters of other trees, as what is discussed in section 5.1.1. Thus, these factors can often lead to difficulty in obtaining accurate height. However, despite these difficulties, there are two aspen trees and one birch tree that had low differences in height, around 20 cm. These trees were likely to have good view conditions during the validation measurements, which could have contributed to a more accurate height estimation.

The comparison of crown diameter between the derived TLS measurement and field measurement was less noticeable (figure 21). The field measurement of crown diameter was conducted using tape measurements, providing an average estimation. In contrast, the TLS measurement of crown diameter provided to be more precise measurements using digital tools in CloudCompare software. The digital approach allowed for greater control and visibility of the individual trees, resulting in more accurate measurements. However, it is still important to notice that the method for crown diameter can still be further improved to minimize the source of error as discussed in 5.1.1.

For instance, Kükenbrink et al. (2021) argued that their findings of crown diameter from the TLS measurement are well correlated with the field measurements with an RMSE of 1.59 m, compared to this study with an RMSE of 0.94 m. One important aspect to take note is the sample size differences, wherein the authors had a larger sample size of 55 trees, which allows for more tree variability, and could have contributed to more robust and accurate results. Furthermore, the authors utilized a rangefinder instrument for their measurement, which may offer higher accuracy compared to tape measurements in the field. This suggests that a large sample size and considering the use of a rangefinder instrument would result in a more robust and accurate AGB estimation and more reliable comparisons between TLS and field measurements of crown diameter.

5.2.2 Volume estimation, modelling of tree structure, and AGB estimation

The derived QSMs have been shown to be accurate and reliable in extracting volume and capturing detailed internal tree structures from segmented tree clouds (figure 17-19). While the QSMs were seen to be reliable, certain challenges still arose during the processing steps that could have contributed to highly time-consuming process when obtaining the desired results.

One notable aspect is the different approaches in generating QSMs for different tree species, reflecting the nature of tree structure and characteristics. For instance, the birch tree has an irregular complex structure and can contribute to some difficulties in generating QSM, depending on the quality of the tree clouds (appendix C). This implication could also contribute to lower CCC and higher CV(RMSE). The displayed birch tree has clustered twigs and potential noise from the points, often associated with environmental factors like wind conditions during the scanning process over time. However, the quality of the point cloud could be improved by increasing the scan mode to high detail during scan processing, but can be more time-consuming in the field.

Despite these challenges, the derived QSMs have provided to be effective for estimating AGB using volume and wood density. Additionally, it can be used for visualization purposes. The detailed information within the QSMs internal tree structure could also be useful for future researches to understand its growth patterns and structure. However, further refining and adjustment of parameters from the steps of QSMs for different tree species are necessary to enhance its overall accuracy and reliability (5.1.2).

The TLS AGB estimation, from QSM volume and wood density (equation 1), and the field AGB estimation using DBH-based tree species equation (equations 2 and 3) have shown to be in great agreement and have relatively low RMSE (figure 22). The near-perfect agreement indicated by the CCC value of 0.997 and the low CV(RMSE) of 7.667% suggests that the model provides an accurate estimation of AGB. However, by observing the results, the TLS AGB estimation tended to be underestimated compared to the field AGB estimation, indicating an overestimation of AGB from the field data.

Similarly, the comparison between TLS AGB estimation and the DBH-based tree-specific equation from the extracted TLS trees shows a high level of agreement with relatively low RMSE (figure 23). The CCC value is slightly lower than the first comparison but still

indicates a strong agreement between the TLS AGB estimation and the TLS validation data. However, the higher CV(RMSE) of 12.881% indicates a greater variation in the estimation. This could be contributed to the significant differences for certain trees, both birch and aspen, indicating over- and underestimating TLS AGB compared to the TLS validation data.

One possible factor that could have contributed to this discrepancy is that the allometric equations used in the field measurement and derived TLS validation rely on DBH measurements. Large trees usually have large DBH, and rarely have been harvested and measured, which could contribute to the overestimation of AGB (Stephenson et al., 2014). This is not surprising, considering that only DBH is utilized for the allometric equations and may not fully capture the variations in AGB for large trees. Therefore, limited availability of data from large trees, and reliance on DBH measurement can lead to overestimation of AGB for large trees from the validation data.

Another possibility is that the size of the crown can also influence AGB. For instance, one birch tree had a significant difference from derived TLS AGB data and TLS validation data, and this was related to the same birch tree as discussed earlier (appendix C). This highlights the importance of considering crown characteristics for estimating AGB (Goodman et al., 2014), as the variations in AGB estimation can be affected by large crown sizes.

Overall, this highlights the importance of utilizing TLS AGB estimation derived from QSMs volume with wood density, particularly for large trees or trees with large crowns. For instance, the QSM-derived parameters used for allometric models could provide a more accurate estimation of AGB across tree species, due to the ability to capture detailed complex characteristics and structure of trees. In contrast, traditional allometric models generally rely on simple parameters, such as DBH, which might not capture the complexity of large trees or large crown sizes. Furthermore, the information derived from the internal structure of trees, such as DBH, crown area, and height, gives the possibility to refine or develop a new allometric model for more robust and accurate AGB estimation. This could be valuable for ecology research to study the tree growth pattern and provide accurate visualization and analysis of forest ecosystems.

6 Conclusions

The study utilized TLS technology and analyzed the data collected using QSM for estimating AGB of aspen and birch trees. The findings from the results and discussion show a strong agreement between TLS-derived AGB estimation using QSM and wood density, and both field AGB estimation and TLS validation using the DBH-based tree species equation. While the overall results are consistent and reliable, small underestimations for large DBH values are highlighted due to the limitation of relying on DBH measurement. These findings could be affected by factors such as large DBH, crown size distribution, and over- or underestimated cylinders from QSM.

The accuracy of TLS-derived DBH and field measurement is in good agreement, although improvements could be done for a more robust estimation. In addition, the accuracy of height measurements varied, influenced by factors such as limitations from conducting the field measurements and environmental conditions, such as rough terrain, dense vegetation, and strong winds. The derived QSMs from TLS data provided to be reliable for volume estimation and analyzing the internal structures of trees, despite the difficulties from processing. However, QSM is still in need of further refinement for a more accurate and robust estimation.

In general, the importance of utilizing TLS data for AGB estimation is highlighted for large trees and in particular trees with large crowns. Additionally, the information from the internal structure of the tree can be integrated into refining or developing new allometric models for more accurate and robust AGB estimation. Moreover, the QSMs have the potential to be reliable for other purposes, such as visualization and ecology research, considering the detailed information they can provide. Importantly, the finding in this study illustrates the potential of TLS and QSM for accurate and reliable AGB estimation, providing valuable validation purposes, for instance by remote sensing researchers. By addressing these challenges, a more robust and accurate AGB estimation can be achieved for future studies.

7 References

Calders, K., Adams, J., Armston, J., Bartholomeus, H., Bauwens, S., Bentley, L. P., Chave, J., Danson, F. M., Demol, M., Disney, M., Gaulton, R., Krishna Moorthy, S. M., Levick, S. R., Saarinen, N., Schaaf, C., Stovall, A., Terryn, L., Wilkes, P., & Verbeeck, H. (2020). Terrestrial laser scanning in forest ecology: Expanding the horizon. *Remote Sensing of Environment*, *251*, 112102. https://doi.org/10.1016/J.RSE.2020.112102

Calders, K., Newnham, G., Burt, A., Murphy, S., Raumonen, P., Herold, M., Culvenor, D., Avitabile, V., Disney, M., Armston, J., & Kaasalainen, M. (2015). Nondestructive estimates of above-ground biomass using terrestrial laser scanning. *Methods in Ecology and Evolution*, *6*(2), 198–208. https://doi.org/10.1111/2041-210X.12301

Chave, J., Coomes, D., Jansen, S., Lewis, S. L., Swenson, N. G., & Zanne, A. E. (2009). Towards a worldwide wood economics spectrum. *Ecology Letters*, *12*(4), 351–366. https://doi.org/10.1111/J.1461-0248.2009.01285.X

Chave, J., Réjou-Méchain, M., Búrquez, A., Chidumayo, E., Colgan, M. S., Delitti, W. B. C., Duque, A., Eid, T., Fearnside, P. M., Goodman, R. C., Henry, M., Martínez-Yrízar, A., Mugasha, W. A., Muller-Landau, H. C., Mencuccini, M., Nelson, B. W., Ngomanda, A., Nogueira, E. M., Ortiz-Malavassi, E., … Vieilledent, G. (2014). Improved allometric models to estimate the aboveground biomass of tropical trees. *Global Change Biology*, *20*(10), 3177–3190. https://doi.org/10.1111/GCB.12629

Chazdon, R., & Brancalion, P. (2019). Restoring forests as a means to many ends. In *Science* (Vol. 364, Issue 6448, pp. 24–25). American Association for the Advancement of Science. https://doi.org/10.1126/science.aax9539

Danson, F. M., Disney, M. I., Gaulton, R., Schaaf, C., & Strahler, A. (2018). The terrestrial laser scanning revolution in forest ecology. *Interface Focus*, *8*(2). https://doi.org/10.1098/RSFS.2018.0001

Demol, M., Verbeeck, H., Gielen, B., Armston, J., Burt, A., Disney, M., Duncanson, L., Hackenberg, J., Kükenbrink, D., Lau, A., Ploton, P., Sewdien, A., Stovall, A., Takoudjou, S. M., Volkova, L., Weston, C., Wortel, V., & Calders, K. (2022). Estimating forest above-ground biomass with terrestrial laser scanning: Current status and future directions. In *Methods in Ecology and Evolution* (Vol. 13, Issue 8, pp. 1628–1639). British Ecological Society. https://doi.org/10.1111/2041-210X.13906

Fan, G., Xu, Z., Wang, J., Nan, L., Xiao, H., Xin, Z., & Chen, F. (2022). Plot-level reconstruction of 3D tree models for aboveground biomass estimation. *Ecological Indicators*, *142*, 109211. https://doi.org/10.1016/J.ECOLIND.2022.109211

Fekry, R., Yao, W., Cao, L., & Shen, X. (2022). Ground-based/UAV-LiDAR data fusion for quantitative structure modeling and tree parameter retrieval in subtropical planted forest. *Forest Ecosystems*, *9*, 100065. https://doi.org/10.1016/J.FECS.2022.100065

GlobAllomeTree. (n.d.). Retrieved May 16, 2023, from http://www.globallometree.org/

Gonzalez de Tanago, J., Lau, A., Bartholomeus, H., Herold, M., Avitabile, V., Raumonen, P., Martius, C., Goodman, R. C., Disney, M., Manuri, S., Burt, A., & Calders, K. (2018). Estimation of above-ground biomass of large tropical trees with terrestrial LiDAR. *Methods in Ecology and Evolution*, *9*(2), 223–234. https://doi.org/10.1111/2041-210X.12904

Goodman, R. C., Phillips, O. L., & Baker, T. R. (2014). The importance of crown dimensions to improve tropical tree biomass estimates. *Ecological Applications*, *24*(4), 680–698. https://doi.org/10.1890/13-0070.1

Gunnarsson, A., & Lorentzon, K. (2017). *Vård och utvecklingsplan för arboretet Valls Hage i Gävle Institutionen för Landskapsarkitektur, planering och förvaltning i samarbete med Samhällsbyggnad Gävle Sveriges lantbruksuniversitet Fakulteten för landskapsarkitektur, trädgårds-och växtproduktionsvetenskap*.

Hackenberg, J., Disney, M., & Bontemps, J.-D. (2022). Gaining insight into the allometric scaling of trees by utilizing 3d reconstructed tree models - a SimpleForest study. *BioRxiv*, 2022.05.05.490069. https://doi.org/10.1101/2022.05.05.490069

Hackenberg, J., Wassenberg, M., Spiecker, H., & Sun, D. (2015). Non Destructive Method for Biomass Prediction Combining TLS Derived Tree Volume and Wood Density. *Forests 2015, Vol. 6, Pages 1274-1300*, *6*(4), 1274–1300. https://doi.org/10.3390/F6041274

Houghton, R. A., Hall, F., & Goetz, S. J. (2009). Importance of biomass in the global carbon cycle. *Journal of Geophysical Research: Biogeosciences*, *114*(G2), 0–03. https://doi.org/10.1029/2009JG000935

Jan, H., Kim, C., Demol, M., Raumonen, P., Piboule, A., & Mathias, D. (2021). SimpleForest - a comprehensive tool for 3d reconstruction of trees from forest plot point clouds. *BioRxiv*, 2021.07.29.454344. https://doi.org/10.1101/2021.07.29.454344

Johansson, T. (1999a). Biomass equations for determining fractions of European aspen growing on abandoned farmland and some practical implications. *Biomass and Bioenergy*, *17*(6), 471–480. https://doi.org/10.1016/S0961-9534(99)00073-2

Johansson, T. (1999b). Biomass equations for determining fractions of pendula and pubescent birches growing on abandoned farmland and some practical implications. *Biomass and Bioenergy (United Kingdom)*. https://doi.org/10.3/JQUERY-UI.JS

Kükenbrink, D., Gardi, O., Morsdorf, F., Thürig, E., Schellenberger, A., & Mathys, L. (2021). Above-ground biomass references for urban trees from terrestrial laser scanning data. *Annals of Botany*, *128*(6), 709–724. https://doi.org/10.1093/AOB/MCAB002

Kumar, L., & Mutanga, O. (2017). Remote Sensing of Above-Ground Biomass. *Remote Sensing 2017, Vol. 9, Page 935*, *9*(9), 935. https://doi.org/10.3390/RS9090935

Kuyah, S., Dietz, J., Muthuri, C., Jamnadass, R., Mwangi, P., Coe, R., & Neufeldt, H. (2012). Allometric equations for estimating biomass in agricultural landscapes: II. Belowground biomass. *Agriculture, Ecosystems & Environment*, *158*, 225–234. https://doi.org/10.1016/J.AGEE.2012.05.010

Ledley, T. S., Sundquist, E. T., Schwartz, S. E., Hall, D. K., Fellows, J. D., & Killeen, T. L. (1999). Climate change and greenhouse gases. *Eos*, *80*(39). https://doi.org/10.1029/99EO00325

Liang, X., Kankare, V., Hyyppä, J., Wang, Y., Kukko, A., Haggrén, H., Yu, X., Kaartinen, H., Jaakkola, A., Guan, F., Holopainen, M., & Vastaranta, M. (2016). Terrestrial laser scanning in forest inventories. *ISPRS Journal of Photogrammetry and Remote Sensing*, *115*, 63–77. https://doi.org/10.1016/J.ISPRSJPRS.2016.01.006

Liang, X., Litkey, P., Hyyppä, J., Kaartinen, H., Vastaranta, M., & Holopainen, M. (2012). Automatic stem mapping using single-scan terrestrial laser scanning. *IEEE Transactions on Geoscience and Remote Sensing*, *50*(2), 661–670. https://doi.org/10.1109/TGRS.2011.2161613

Lin, L. I.-K. (1989). A Concordance Correlation Coefficient to Evaluate Reproducibility. In *Source: Biometrics* (Vol. 45, Issue 1).

McMichael, A. J., Woodruff, R. E., & Hales, S. (2006). Climate change and human health: present and future risks. *The Lancet*, *367*(9513), 859–869. https://doi.org/10.1016/S0140-6736(06)68079-3

Miah, M. D., Islam, K. N., Kabir, M. H., & Koike, M. (2020). Allometric models for estimating aboveground biomass of selected homestead tree species in the plain land Narsingdi district of Bangladesh. *Trees, Forests and People*, *2*, 100035. https://doi.org/10.1016/J.TFP.2020.100035

Návar, J. (2009). Allometric equations for tree species and carbon stocks for forests of northwestern Mexico. *Forest Ecology and Management*, *257*(2), 427–434. https://doi.org/10.1016/J.FORECO.2008.09.028

Newnham, G. J., Armston, J. D., Calders, K., Disney, M. I., Lovell, J. L., Schaaf, C. B., Strahler, A. H., & Mark Danson, F. (2015). Terrestrial laser scanning for plot-scale forest measurement. *Current Forestry Reports*, *1*(4), 239–251. https://doi.org/10.1007/s40725-015-0025-5

Persson, H. J., Ekström, M., & Ståhl, G. (2022). Quantify and account for field reference errors in forest remote sensing studies. *Remote Sensing of Environment*, *283*. https://doi.org/10.1016/j.rse.2022.113302

Pragasan, L. A. (2020). *Tree carbon stock and its relationship to key factors from a tropical hill forest of Tamil Nadu, India*. https://doi.org/10.1080/24749508.2020.1742510

Raumonen, P., Kaasalainen, M., Markku, Å., Kaasalainen, S., Kaartinen, H., Vastaranta, M., Holopainen, M., Disney, M., & Lewis, P. (2013). Fast Automatic Precision Tree Models from Terrestrial Laser Scanner Data. *Remote Sensing 2013, Vol. 5, Pages 491-520*, *5*(2), 491–520. https://doi.org/10.3390/RS5020491

Stephenson, N. L., Das, A. J., Condit, R., Russo, S. E., Baker, P. J., Beckman, N. G., Coomes, D. A., Lines, E. R., Morris, W. K., Rüger, N., Álvarez, E., Blundo, C., Bunyavejchewin, S., Chuyong, G., Davies, S. J., Duque, Á., Ewango, C. N., Flores, O., Franklin, J. F., … Zavala, M. A. (2014). Rate of tree carbon accumulation increases continuously with tree size. *Nature 2014 507:7490*, *507*(7490), 90–93. https://doi.org/10.1038/nature12914

Terryn, L., Calders, K., Åkerblom, M., Bartholomeus, H., Disney, M., Levick, S., Origo, N., Raumonen, P., & Verbeeck, H. (2023). Analysing individual 3D tree structure using the R package ITSMe. *Methods in Ecology and Evolution*, *14*(1), 231–241. https://doi.org/10.1111/2041-210X.14026

Wandinger, U. (2005). Introduction to Lidar. *Lidar*, 1–18. https://doi.org/10.1007/0-387-25101-4_1

Wang, L., Zhou, X., Zhu, X., Dong, Z., & Guo, W. (2016). Estimation of biomass in wheat using random forest regression algorithm and remote sensing data. *The Crop Journal*, *4*(3), 212–219. https://doi.org/10.1016/J.CJ.2016.01.008

Wehr, A., & Lohr, U. (1999). Airborne laser scanning—an introduction and overview. *ISPRS Journal of Photogrammetry and Remote Sensing*, *54*(2–3), 68–82. https://doi.org/10.1016/S0924-2716(99)00011-8

Xu, D., Wang, H., Xu, W., Luan, Z., & Xu, X. (2021). LiDAR applications to estimate forest biomass at individual tree scale: Opportunities, challenges and future perspectives. *Forests*, *12*(5). https://doi.org/10.3390/f12050550

Appendix A. Differences in DBH between TLS-derived and field measurement.

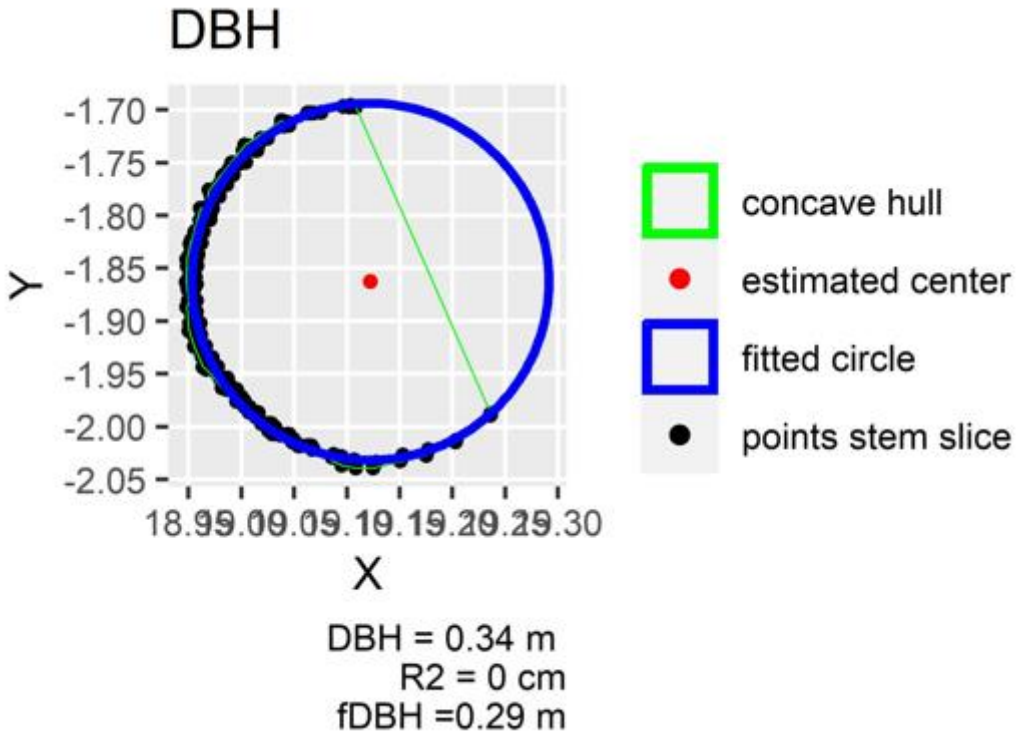

Appendix B. Spherefollowing processing step in SimpleForest tool.

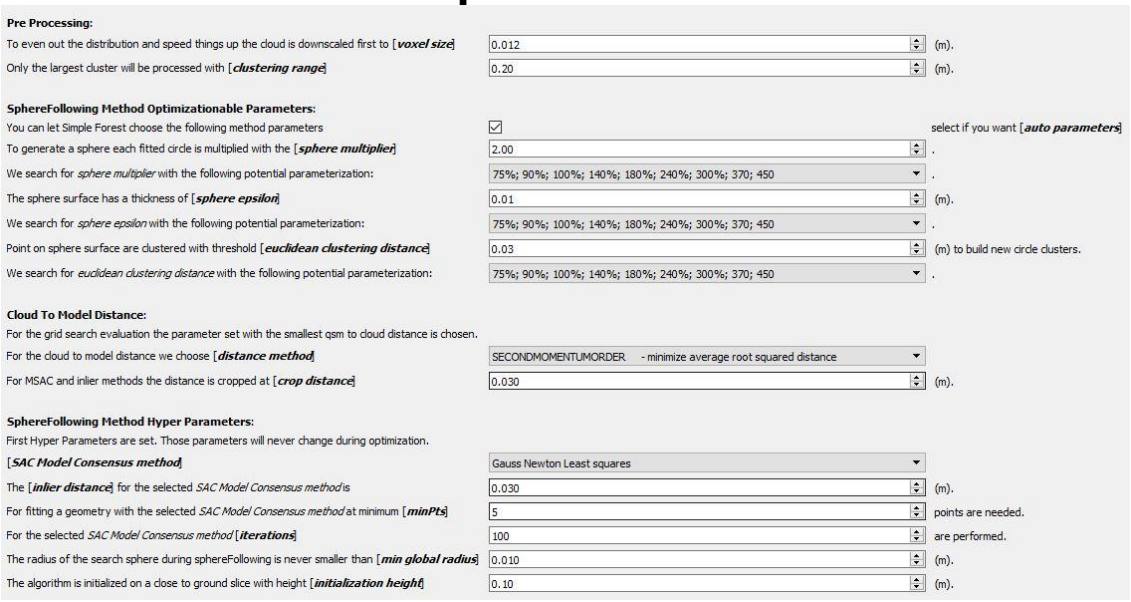

Appendix C. Single Birch tree with high irregular complex structure (Left tree cloud) (right QSM)